Passivity-based switching control of flexible-joint complementarity mechanical systems

Irinel-Constantin Morarescu, Bernard Brogliato, Said Haad

INSTITUT NATIONAL DE RECHERCHE EN INFORMATIQUE ET EN AUTOMATIQUE

Passivity-based switching control of flexible-joint complementarity mechanical systems

Irinel–Constantin Morărescu — Bernard Brogliato — Said Hadd

N° 6739

Novembre 2008

Thème NUM

Rapport de recherche

ISSN 0249-6399 ISRN INRIA/RR--6739--FR+ENG

Passivity-based switching control of flexible-joint complementarity mechanical systems

Irinel–Constantin Morărescu[*, †] , Bernard Brogliato[‡, †] , Said Hadd[§, ¶]

Thème NUM — Systèmes numériques
Équipe-Projet BIPOP

Rapport de recherche n° 6739 — Novembre 2008 — 38 pages

Abstract: In this study one considers the tracking control problem of a class of nonsmooth Lagrangian systems with flexible joints and subject to frictionless unilateral constraints. The task under consideration consists of a succession of free-motion and constrained-motion phases. A particular attention is paid to impacting and detachment phases. A passivity-based switching controller that allows to extend the stability analysis described in our previous works to the case of systems with lumped flexibilities, is proposed. Numerical tests show the effectiveness of the controller.

Key-words: Flexible joints, Passivity-based control, Nonsmooth systems, Lagrangian systems, Complementarity problem.

[*] `constantin.morarescu@inrialpes.fr`
[†] INRIA, Inovallée, 655 avenue de l'Europe, 38330, Montbonnot, France.
[‡] `bernard.brogliato@inrialpes.fr`
[§] `s.hadd@liv.ac.uk`
[¶] Department of Electrical Engineering and Electronics, the University of Liverpool, Brownlow Hill Liverpool, L69 3GJ, United Kingdom.

Centre de recherche INRIA Grenoble – Rhône-Alpes
655, avenue de l'Europe, 38334 Montbonnot Saint Ismier
Téléphone : +33 4 76 61 52 00 — Télécopie +33 4 76 61 52 52

Commande passive pour la poursuite de trajectoires dans les systèmes Lagrangiens non-réguliers multi-contraintes

Résumé : Dans cette étude, on considère le problème de la commande pour assurer la poursuite des trajectoires pour une classe de systèmes Lagrangiens non-réguliers avec des articulations flexibles et soumis à des contraintes unilatérales sans frottement. La tâche typique considerée consiste en une succession de phases de mouvement libre et des phases de mouvement contraint. Une attention particuliére est accordée aux phases de transition avec impacts et aux phases de détachement. Une commande basée sur la passivité permet d'étendre l'analyse de stabilité presentée dans nos travaux précédents au cas des systèmes avec flexibilités. Des tests numériques montrent l'efficacité de la commande.

Mots-clés : Articulations flexible, Commande basée sur la passivité, Systèmes non-réguliers, Systèmes Lagrangiens, Problème de complémentarité.

Contents

1 Introduction

The control of flexible mechanical systems (especially flexible-joint robots) has been a challenging and important subject for the last decades. Considering dynamics that contains impacts due to some unilateral constraints renders the problem even more difficult. Such systems, which consist of three main ingredients (see (1) below) are highly nonlinear nonsmooth dynamical systems. The control of systems undergoing impacts has received attention in the literature [3, 19, 31, 32, 33, 35, 36, 38]. In parallel with such works focusing solely on the collision phase, more general studies concerning the stability and tracking control of nonsmooth unilaterally constrained mechanical systems have been published [6, 7, 8, 9, 12, 17, 20, 21, 22, 25, 26, 27, 28, 34, 39]. Until now these works have been limited to perfectly rigid systems. The consideration of flexibilities seems mandatory. On one hand impacts may damage rigid systems small flexibility, whereas flexibility can reduce the damage by impact absorption [37]. On the other hand, impact phenomena may excite vibrational modes, which is not desirable in practice (see Section 8). Introducing flexibility however is challenging for the control design. One of the main difficulty added in the flexible case is that the backstepping procedure requires the definition of some exogenous trajectory as nonlinear functions of states and other exogenous signals. As a result, the jumps of the "passivity-based" Lyapunov function are more difficult to characterize.

In this work it is shown that the tracking control framework developed in [8, 12] can be adapted to the flexible-joint case, using the passivity-based motion control solutions proposed in [13]. More precisely, this paper focuses on the problem of tracking control of complementarity Lagrangian systems [30], encompassing flexible-joint manipulators subject to frictionless unilateral constraints, whose dynamics may be expressed as:

$$\begin{cases} M(X)\ddot{X} + C(X,\dot{X})\dot{X} + G(X) = K(\theta - X) + \nabla F(X)\lambda \\ J\ddot{\theta} = U + K(X-\theta) \\ 0 \leq \lambda \perp F(X) \geq 0, \\ \text{Collision rule} \end{cases} \tag{1}$$

where $X(\cdot) \in \mathbb{R}^n$ is the vector of rigid links angles, $\theta(\cdot) \in \mathbb{R}^n$ is the vector of motor shaft angles, $M(X) = M^T(X) \in \mathbb{R}^{n\times n}$ is a positive definite inertia matrix, $F(X) \in \mathbb{R}^m$ represents the distance to the constraints, $C(X,\dot{X})$ is the matrix containing Coriolis and centripetal forces, $G(X)$ contains conservative forces, $\lambda \in \mathbb{R}^m$ is the vector of contact forces (or Lagrangian multipliers) associated to the constraints, $J \in \mathbb{R}^{n\times n}$ is the diagonal and constant matrix of actuator inertia reflected to the link side of the gears, $K = K^\top > 0,\ K \in \mathbb{R}^{n\times n}$ represents the stiffness matrix and $U \in \mathbb{R}^n$ is the vector of generalized torque inputs. A vector is considered positive if all its component are positive. For the sake of completeness we precise that ∇ denotes the Euclidean gradient $\nabla F(X) = (\nabla F_1(X), \ldots, \nabla F_m(X)) \in \mathbb{R}^{n\times m}$ where $\nabla F_i(X) \in \mathbb{R}^n$ represents the vector of partial derivatives of $F_i(\cdot)$ w.r.t. the components of X. We assume that the functions $F_i(\cdot)$ are continuously differentiable and that $\nabla F_i(X) \neq 0$ for all X with $F_i(X) = 0$. A constraint i is said to be *active* if $F_i(X) = 0$, and *inactive* if $F_i(X) > 0$.

General notations and definitions. $||\cdot||$ is the Euclidean norm, $b_p \in \mathbb{R}^p$ and $b_{n-p} \in \mathbb{R}^{n-p}$ are the vectors formed with the first p and the last $n-p$ components of $b \in \mathbb{R}^n$, respectively. $N_\Phi(X_p = 0)$ is the normal cone $N_\Phi(X)$ to Φ at X when X satisfies $X_p = 0$; $\lambda_{min}(\cdot)$ and $\lambda_{max}(\cdot)$ represent the smallest and the largest eigenvalues, respectively. The time-derivative of a function $f(\cdot)$ is denoted by $\dot{f}(\cdot)$. For any function $f(\cdot)$ the limit to the right at the instant t will be denoted by $f(t^+)$ and the limit to the left will be denoted by $f(t^-)$ when they exist. A simple jump of the function $f(\cdot)$ at the moment $t = t_\ell$ is denoted $\sigma_f(t_\ell) = f(t_\ell^+) - f(t_\ell^-)$. 0_n is the n-vector with entries 0, and $0_{n\times m}$ is the $n \times m$-zero matrix. I_m is the $m \times m$ identity matrix

Definition 1 *A Linear Complementarity Problem (LCP) with unknown λ is a system: $\lambda \geq 0$, $A\lambda + b \geq 0$, $\lambda^\top(A\lambda + b) = 0$, which is compactly rewritten as $0 \leq \lambda \perp A\lambda + b \geq 0$. Such an LCP has a unique solution for all b if and only if A is a P-matrix [16]. Positive definite matrices (not necessarily symmetric) are P-matrices.*

The admissible domain associated to the system (1) is the closed set Φ where the system can evolve and it is described as follows:

$$\mathbf{\Phi} \triangleq \{(X,\theta) \in \mathbb{R}^{2n} \mid F(X) \geq 0\} = \left(\bigcap_{1\leq i\leq m} \Phi_i\right) \times \mathbb{R}^n,$$

where $\Phi_i = \{X \mid F_i(X) \geq 0\}$. In order to have a well-posed problem with a physical meaning we consider that $\mathbf{\Phi}$ contains at least a closed ball of positive radius. In the sequel $\left(\bigcap_{1\leq i\leq m} \Phi_i\right)$ will be denoted by $\Phi \subset \mathbb{R}^n$.

Definition 2 *A singularity of the boundary $\partial\mathbf{\Phi}$ of $\mathbf{\Phi}$ is the intersection of two or more surfaces $\Sigma_i = \partial\Phi_i\{X \mid F_i(X) = 0\} \times \mathbb{R}^n$.*

The presence of $\partial\mathbf{\Phi}$ may induce some impacts that must be included in the dynamics of the system. It is obvious that $m > 1$ allows both simple impacts (when one constraint is involved) and multiple impacts (when singularities are involved). Let us introduce the following notion of p_ϵ-impact.

Definition 3 *Let $\epsilon \geq 0$ be a fixed real number. We say that a p_ϵ-impact occurs at the instant t if*

$$||F_I(X(t))|| \leq \epsilon, \quad \prod_{i\in I} F_i(X(t)) = 0$$

where $I \subset \{1, \ldots, m\}$, $card(I) = p$, and $F_I(X(t))$ is the $p-$vector with entries $F_i(X(t))$, $i \in I$.

If $\epsilon = 0$ all p surfaces Σ_i, $i \in I$ are struck simultaneously. When $\epsilon > 0$ the system collides $\partial\mathbf{\Phi}$ in a neighborhood of the intersection $\bigcap_{i\in I} \Sigma_i$.

Definition 4 *[30] The tangent cone to $\mathbf{\Phi} = \Phi \times \mathbb{R}^n$ at $x = (x_1, x_2) \in \mathbb{R}^n \times \mathbb{R}^n$ is:*

$$\begin{aligned} T_{\mathbf{\Phi}}(x) &= \{(z_1, z_2) \in \mathbb{R}^n \times \mathbb{R}^n \mid z_1^\top \nabla F_i(x_1) \geq 0, \forall i \in S(x_1)\} \\ &= \{z_1 \in \mathbb{R}^n \mid z_1^\top \nabla F_i(x_1) \geq 0, \forall i \in S(x_1)\} \times \mathbb{R}^n \equiv T_\Phi(x_1) \times \mathbb{R}^n \end{aligned}$$

where $S(x_1) \triangleq \{i \in \{1, \ldots, m\} \mid F_i(x_1) \leq 0\}$. When $x \in \mathbf{\Phi} \setminus \partial\mathbf{\Phi}$ one has $S(x_1) = \emptyset$ and $T_{\mathbf{\Phi}}(x) = \mathbb{R}^{2n}$. The normal cone to $\mathbf{\Phi}$ at x is defined as the polar cone to $T_{\mathbf{\Phi}}(\cdot)$:

$$\begin{aligned} N_{\mathbf{\Phi}}(x) &= \{Y = (y_1, y_2) \in \mathbb{R}^n \times \mathbb{R}^n \mid \forall z \in T_{\mathbf{\Phi}}(x), y^\top z \leq 0\} \\ &= \{y_1 \in \mathbb{R}^n \mid \forall z_1 \in T_\Phi(x_1), y_1^\top z_1 \leq 0\} \times \{0_n\} \equiv N_\Phi(x_1) \times \{0_n\} \end{aligned}$$

The collision (or restitution) rule in (1), is a relation between the post-impact velocity and the pre-impact velocity. Among the various models of collision rules, Moreau's rule is an extension of Newton's law which is energetically consistent and is numerically tractable [1]. For these reasons throughout this paper the collision rule will be defined by Moreau's relation [30]:

$$\begin{aligned} \dot{X}(t_\ell^+) &= (1+e) \operatorname*{arg\,min}_{z_1 \in T_\Phi(X(t_\ell))} \frac{1}{2}[z_1 - \dot{X}(t_\ell^-)]^T \times M(X(t_\ell))[z_1 - \dot{X}(t_\ell^-)] - e\dot{X}(t_\ell^-) \\ \dot{\theta}(t_\ell^+) &= (1+e) \operatorname*{arg\,min}_{z_2 \in \mathbb{R}^n} \frac{1}{2}[z_2 - \dot{\theta}(t_\ell^-)]^T \times J[z_2 - \dot{\theta}(t_\ell^-)] - e\dot{\theta}(t_\ell^-) = \dot{\theta}(t_\ell^-) \end{aligned} \tag{2}$$

where $\dot{X}(t_\ell^+)$, $\dot{\theta}(t_\ell^+)$ are the post-impact velocities, $\dot{X}(t_\ell^-)$, $\dot{\theta}(t_\ell^-)$ are the pre-impact velocities and $e \in [0, 1]$ is the restitution coefficient[1]. Under mild conditions on the data, the solutions are such that the positions $X(\cdot)$ and $\theta(\cdot)$ are absolutely continuous functions of time, whereas the generalized velocity is right continuous of local bounded variation. Well-posedness results may be found in [15, 23] and references therein. From (2) the following result then holds.

[1]For the sake of simplicity we consider that one has the same restitution coefficient w.r.t. all the surfaces i.e. $e_1 = \ldots = e_m \triangleq e$.

Proposition 1 *The velocity $\dot{\theta}(\cdot)$ is a continuous function of time.*

Another way to prove Proposition 1 (based on the fact that $J(\dot{\theta}(t_k^+) - \dot{\theta}(t_k^-)) = 0$ when the dynamics is written as an equality of measures) can be found in [10, §3.4.1]. The continuity of $\dot{\theta}(\cdot)$ will be used in the stability analysis developed in section 7. We note that in the more complete model where the inertia matrix has off block diagonal elements, then $\dot{\theta}(\cdot)$ jumps at impacts.

Denoting by T the kinetic energy of the system, we can compute the kinetic energy loss at the impact t_ℓ as [23]:

$$T_L(t_\ell) = -\frac{1-e}{2(1+e)}\left[\dot{X}(t_\ell^+) - \dot{X}(t_\ell^-)\right]^T M(X(t_\ell)) \times [\dot{X}(t_\ell^+) - \dot{X}(t_\ell^-)\Big] \leq 0 \quad (3)$$

The structure of the paper is as follows: in Section 2 one presents some basic concepts and necessary prerequisites. Section 4 is devoted to the controller design. In this section one also defines the desired (or ”exogenous”) trajectories entering the dynamics. The desired contact-force that must occur on the phases where the motion is persistemtly constrained, is explicitly defined in Section 5. Section 6 focuses on the strategy for take-off at the end of the constraint phases. The main results related to the closed-loop stability analysis are presented in Section 7. A numerical example obtained with the SICONOS platform and concluding remarks end the paper.

2 Basic concepts

2.1 Typical task

Since the system's dynamics does not change when the number of active constraints decreases one gets the following typical task representation:

$$\begin{gathered}\mathbb{R}^+ = \bigcup_{k\geq 0}\left(\Omega_{2k}^{B_k} \cup I_k^{B_k} \cup \left(\bigcup_{i=1}^{m_k} \Omega_{2k+1}^{B_{k,i}}\right)\right) \\ B_k \subset B_{k,1};\ B_{k+1} \subset B_{k,m_k} \subset B_{k,m_k-1} \subset \dots B_{k,1}\end{gathered} \quad (4)$$

where the superscript B_k represents the set of active constraints during the corresponding motion phase ($B_k = \{i \in \{1,\dots,m\} \mid F_i(X) = 0\}$), and $I_k^{B_k}$ denotes the transient between two Ω_k phases when the number of active constraints increases. We note that $B_k = \emptyset$ corresponds to free-motion. When the number of active constraints decreases no transition phases are needed, thus, for the sake of simplicity and without any loss of generality we replace $\bigcup_{i=1}^{m_k} \Omega_{2k+1}^{B_{k,i}}$ by $\Omega_{2k+1}^{B'_k}$ and the typical task representation simplifies as:

$$\mathbb{R}^+ = \bigcup_{k\geq 0}\left(\Omega_{2k}^{B_k} \cup I_k^{B_k} \cup \Omega_{2k+1}^{B'_k}\right),\ B_k \subset B'_k, \quad B_{k+1} \subset B'_k \quad (5)$$

Since the tracking control problem involves no difficulty during the Ω_k-phases, *the central issue is the study of the passages between them (the design of transition phases I_k and detachment conditions), and the stability of the trajectories evolving along (5)* (i.e. an infinity of cycles). Throughout the paper, the sequence $\Omega_{2k}^{B_k} \cup I_k^{B_k} \cup \Omega_{2k+1}^{B'_k}$ will be referred to as the cycle k of the system's evolution. For robustness reasons, during the transition phases I_k we impose a closed-loop dynamics (containing impacts) that mimics somehow the bouncing-ball dynamics (see e.g. [10]). It is noteworthy that a tangential approach may lead to instability or no stabilization at all on $\partial\phi$ (see for instance Figure 7 in Section 8).

2.2 Well-posedness

Here we shall briefly recall the theorem giving the conditions for the existence and uniqueness of the solution of (1), quoting the result from [4, §3]. First, (1) rewrites more compactly as

$$\left\{\begin{array}{l} \mathcal{M}(\varphi)\ddot{\varphi} + \mathcal{C}(\varphi,\dot{\varphi})\dot{\varphi} + \mathcal{G}(\varphi) + \mathcal{K}\varphi = EU + \nabla H(\varphi)\lambda \\ 0 \le \lambda \perp H(\varphi) \ge 0, \\ \text{Collision rule} \end{array}\right. \tag{6}$$

where $\varphi \triangleq (X^\top, \theta^\top)^\top$, $\mathcal{G}(\varphi) = \begin{pmatrix} G(X) \\ 0_n \end{pmatrix}$, $E = \begin{pmatrix} 0_n \\ I_n \end{pmatrix}$, $\mathcal{K} = \begin{pmatrix} K & -K \\ -K & K \end{pmatrix}$, $\mathcal{M}(\varphi) = \begin{pmatrix} M(X) & 0_n \\ 0_n & J \end{pmatrix}$, $\mathcal{C}(\varphi,\dot{\varphi}) = \begin{pmatrix} C(X,\dot{X}) & 0_n \\ 0_n & 0_n \end{pmatrix}$ and $H : \mathbb{R}^{2n} \mapsto \mathbb{R}^m$, $H(\varphi) = F(X)$.

The existence of the solutions for (6) has been already proved in several works using somehow similar arguments. As we have already mentioned in the introductory section the presence of the impacts induce a discontinuity of the velocity. So to integrate the model we shall take into account the collision rule. Using this collision law one can rewrite (6) as a differential inclusion in term of differential measures defined by LBV functions. Let us define

$$B(\varphi,\dot{\varphi};t) \triangleq EU - [\mathcal{C}(\varphi,\dot{\varphi})\dot{\varphi} + \mathcal{K}\varphi + G(\varphi)].$$

The first equation of (6) becomes

$$\mathcal{M}(\varphi)\ddot{\varphi} = B(\varphi,\dot{\varphi};t) + \nabla H(\varphi)\lambda. \tag{7}$$

To give a meaning to (7) at impact times we shall reformulate this equation in the distributional sense using representation of measures. To this aim let us denote the velocity $v(\cdot)$ that is a right-continuous function of local bounded variation, $v(\cdot)$ is equal almost everywhere to $\dot{\varphi}(\cdot)$, $\varphi(\cdot)$ is absolutely continuous and $\varphi(t) - \varphi(0) = \int_{[0,t]} v(s)ds$. Moreover, we denote by $N_{V(\varphi(t))}(v(t^+))$ the normal cone to the tangent cone $V(\varphi(t))$ at $v(t^+)$, where the cones are as in Definition 4. Then, as shown in [1, 10, 23, 30], the system (6) can be embedded in the measure differential inclusion

$$\left\{\begin{array}{l} -\mathcal{M}(\varphi(t))dv + B(\varphi,\dot{\varphi};t)dt \in N_{T_\Phi(\varphi(t))}(w(t)) \\ w(t) = \frac{v(t^+)+ev(t^-)}{1+e} \end{array}\right. \tag{8}$$

The existence and uniqueness of the solutions is summarized in the following theorem (see [4, §3] for more details).

Theorem 1 *Assume that there exists a function $l \in L^1_{loc}(\mathbb{R},\mathbb{R}_+)$ such that*

$$\|B(\varphi,\dot{\varphi};t)\|_\varphi \le l(t)(1 + d(\varphi,\varphi(0)) + \|v\|_\varphi),$$

where $d(\varphi, \varphi(0))$ is the Riemannian distance and $\| \cdot \|_\varphi$ is the kinetic norm. Then (8) *has a unique global solution (on $\mathbb{R}^+$) with $\varphi(\cdot)$ absolutely continuous, whereas the velocity $v(\cdot)$ is right continuous of locally bounded variation. Moreover, the acceleration is a measure $dv = \{\ddot{\varphi}\}dt + d\mu_a$, where $\{\ddot{\varphi}\}$ is a Lebesgue integrable function, and $d\mu_a$ is an atomic measure with a countable set of atoms on any compact time interval* (atoms coincide with impact times).

2.3 System properties

This paragraph is devoted to some properties that will play an important role in the stability analysis of the system (6). First one notes that $C(X, \dot{X})$ is not unequivocally defined by the term $C(X, \dot{X})\dot{X}$. Nevertheless the kinetic energy defines a Riemannian structure on the configuration space that allows to introduce the elements of $C(X, \dot{X})$ via the Christoffel symbols Γ_{ijk} associated to the corresponding metric. Precisely one considers

$$C_{ij}(X, \dot{X}) = \sum_{k=1}^{n} \Gamma_{ijk} \dot{X}_k, \quad \Gamma_{ijk} = \frac{1}{2}\left(\frac{\partial M_{ij}(X)}{\partial X_k} + \frac{\partial M_{ik}(X)}{\partial X_j} - \frac{\partial M_{kj}(X)}{\partial X_i} \right) \tag{9}$$

Definition 5 *For a real valued function $f : \mathbb{R}^+ \mapsto \mathbb{R}$ one denotes by $S(f)$ the set of all real valued function $g : \mathbb{R}^+ \mapsto \mathbb{R}$ such that there exists a positive real constant $0 < c < \infty$ satisfying $g(t) \leq cf(t)$, $\forall t \geq 0$. One writes $g \in S(1) \equiv L^\infty$ if $f(t) = 1$, $\forall t \geq 0$.*

Property 1 *The matrix $\left[\frac{d}{dt}M(X)\right] - 2C(X, \dot{X})$ is skew-symmetric and $\dot{M}(X) \triangleq \frac{d}{dt}M(X) = C(X, \dot{X}) + C^\top(X, \dot{X})$. Furthermore the matrix $C(X, \dot{X})$ is a smooth function of X and $\dot{X}$ with the well-known properties:*

$$||C(X, \dot{X})|| \in S(||\dot{X}||) \tag{10}$$

and

$$C(X, Y)Z = C(X, Z)Y, \quad \forall\, X, Y, Z \in \mathbb{R}^n \tag{11}$$

Property 2 *The conservative forces vector $G(X)$ is such that $\left|\left|\frac{\partial G(X)}{\partial X}\right|\right| \in S(1)$ which implies by the mean value theorem $||G(X_1) - G(X_2)|| \in S(||X_1 - X_2||)$, $\quad \forall X_1, X_2 \in \mathbb{R}^n$.*

Property 3 *The matrix $C(X, \dot{X})$ is such that*

$$\left|\left|\frac{\partial C(X, \dot{X})}{\partial X}\right|\right| \in S(||\dot{X}||), \quad \left|\left|\frac{\partial C(X, \dot{X})}{\partial \dot{X}}\right|\right| \in S(1)$$

The properties 2 and 3 rely on the fact that $G(X)$ is formed by linear or trigonometric function $(\sin, \cos)$ of the link variables while the components of $C(X, \dot{X})$ are obtained as product of affine functions of the link velocities and trigonometric function $(\sin, \cos)$ of the link variables.

2.4 Stability analysis criteria

The system (1) is a complex nonsmooth and nonlinear dynamical system. A stability framework for this type of systems has been proposed in [12] and extended in [8, 29]. This is an extension of the Lyapunov second method adapted to closed-loop mechanical systems with unilateral constraints. Since we use this criterion in the following tracking control strategy it is worth to clarify the framework and to introduce some definitions. Let us define Ω as the complement in $\mathbb{R}_+$ of $I = \bigcup_{k\geq 0} I_k^{B_k}$ and assume that the Lebesgue measure of Ω, denoted $\lambda[\Omega]$, equals infinity. Let us denote by φ_d the signal playing the role of the desired trajectory (see Section 4). Consider $x(\cdot)$ the state of the closed-loop system in (6) with some feedback controller $U(\varphi, \dot{\varphi}, \varphi_d, \dot{\varphi}_d, \ddot{\varphi}_d)$.

Definition 6 (Weakly Stable System [8]) *The closed loop system is called weakly stable if for each $\epsilon > 0$ there exists $\delta(\epsilon) > 0$ such that $||x(0)|| \leq \delta(\epsilon) \Rightarrow ||x(t)|| \leq \epsilon$ for all $t \geq 0,\ t \in \Omega$. The system is asymptotically weakly stable if it is weakly stable and $\lim_{t\in\Omega,\, t\to\infty} x(t) = 0$. Finally, practical weak stability holds if there exists $0 < R < +\infty$ and $t^* < +\infty$ such that $||x(t)|| < R$ for all $t > t^*,\ t \in \Omega$.*

Consider $I_k^{B_k} \triangleq [\tau_0^k, t_f^k]$ and $V(\cdot)$ such that there exists strictly increasing functions $\alpha(\cdot)$ and $\beta(\cdot)$ satisfying the conditions: $\alpha(0) = 0,\ \beta(0) = 0$ and $\alpha(||x||) \leq V(x,t) \leq \beta(||x||)$. In the sequel, we consider that for each cycle the sequence of impact instants $\{t_\ell^k\}_{\ell\geq 0}$ has an accumulation point t_∞^k. We note that a finite accumulation period (i.e. $t_\infty^k < +\infty$) implies that $e < 1$ (in [5] it is shown that $e = 1$ implies that $t_\infty^k = +\infty$).

The following criterion is inspired from [8] and [29], and will be used to study the stability of the system (1).

Proposition 2 (Weak Stability) *Assume that the task admits the representation (5) and that*

a) $\lambda[I_k^{B_k}] < +\infty, \quad \forall k \in \mathbb{N}$,

b) *outside the impact accumulation phases $[t_0^k, t_\infty^k]$ one has $\dot{V}(x(t),t) \leq -\gamma V(x(t),t)$ for some constant $\gamma > 0$,*

c) *the system is initialized on Ω_0 such that $V(\tau_0^0) \leq 1$,*

d) $V(t_\infty^k) \leq \rho^* V(\tau_0^k) + \xi$ *where* $\rho^*,\ \xi \in \mathbb{R}_+$.

Then $V(\tau_0^k) \leq \delta(\gamma,\xi),\ \forall k \geq 1$ where $\delta(\gamma,\xi)$ is a function that can be made arbitrarily small by increasing either the value of γ or the length of the time interval $[t_\infty, t_f]$. Thus, the system is practically weakly stable with $R = \alpha^{-1}(\delta(\gamma,\xi))$.

Proof: From assumption **(b)** one has

$$V(t_f^k) \leq V(t_\infty^k) e^{-\gamma(t_f^k - t_\infty^k)}$$

and using condition **(d)** and **(c)** we arrive at

$$V(t_f^k) \leq e^{-\gamma(t_f^k - t_\infty^k)}\left(\rho^* V(\tau_0^k) + \xi\right) \leq e^{-\gamma(t_f^k - t_\infty^k)}(\rho^* + \xi) \triangleq \delta(\gamma,\xi)$$

Assumption **(b)** also guarantees that $V(\tau_0^{k+1}) \leq V(t_f^k)$ and thus $V(\tau_0^k) \leq \delta(\gamma,\xi),\ \forall k \geq 1$. The term $\delta(\gamma,\xi)$ can be made as small as desired increasing either γ or the length of the interval $[t_\infty^k, t_f^k]$. The proof is completed by the relation $\alpha(||x||) \leq V(x,t),\ \forall x,\ t$.

Remark 1 *It is worth to point out the local character of the stability criterion in Proposition 2. This is firstly due to condition* **(c)** *and secondly by the synchronization constraints of the control law and the motion phase of the system (see (5) and (19)-(20) below). The weak stability relies on almost non-increasing functions, as introduced in [12] (see also [14]). Condition* **(d)** *means that the impacts may be considered as a kind of disturbance that can be suitably upper bounded. This is certainly the most crucial point in Proposition 2.*

3 Change of generalized coordinates

Let us rewrite (6) into the generalized coordinates introduced in [24]. We shall assume that there exists a continuously differentiable function $\xi : \mathbb{R}^{n-m} \to \mathbb{R}^m$ such that

$$F(\xi(X_2), X_2, \theta) \geq 0 \quad \text{for any} \quad X_2 \in \mathbb{R}^{n-m},\, \theta \in \mathbb{R}^n.$$

Now if we decompose $\varphi = (X_1^\top, X_2^\top, \theta^\top)^\top \in \mathbb{R}^{2n}$ with $X_1 \in \mathbb{R}^m$ and $X_2 \in \mathbb{R}^{n-m}$ then one can define an invertible transformation $\Gamma : \mathbb{R}^{2n} \to \mathbb{R}^{2n}$ by setting

$$\Gamma(\varphi) = (X_1^\top - \xi(X_2)^\top, X_2^\top, \theta^\top)^\top \triangleq (q^\top, \theta^\top)^\top. \tag{12}$$

Throughout the rest of this paper we denote by $Q(\cdot)$ the inverse of $\Gamma(\cdot)$. Thus, denoting $\psi = (q^\top, \theta^\top)^\top$ one has

$$\varphi = Q(\psi) = \left(q_1^\top + \xi(q_2)^\top, q_2^\top, \theta^\top\right)^\top,$$

where $q \triangleq (q_1^\top, q_2^\top)^\top$ with $q_1 \in \mathbb{R}^m$ and $q_2 \in \mathbb{R}^{n-m}$.Let us also denote by $Q_1(\psi) = \left(q_1^\top + \xi(q_2)^\top, q_2^\top\right)^\top$ and $Q_2(\psi) = \theta$ the projections on the first n and the last n components of $Q(\psi)$ respectively. The Jacobian matrix of $Q(\cdot)$ is given by

$$\Pi(q) \triangleq \left(\begin{array}{cc|c} I_m & \frac{\partial \xi}{\partial q_2}(q_2) & 0_{n\times n} \\ 0_{(n-m)\times m} & I_{n-m} & 0_{n\times n} \\ \hline \multicolumn{2}{c|}{0_{n\times n}} & I_n \end{array}\right), \quad \psi \in \mathbb{R}^{2n}.$$

For $\varphi = Q(\psi)$ we define the following operators

$$\begin{cases} \mathbf{M}(\psi) \triangleq \Pi(q)^\top \mathcal{M}(Q(\psi))\Pi(q) \\ \mathbf{C}(\psi, \dot\psi) \triangleq \Pi(q)^\top \left[\mathcal{C}(Q(\psi), \Pi(q)\dot q)\Pi(q) + \mathcal{M}(Q(\psi))\dot\Pi(\psi)\right] \\ \mathbb{K}(\cdot;\psi) \triangleq \Pi(q)^\top \mathcal{K} Q(\cdot) \\ \mathbf{G}(\cdot;\psi) \triangleq \Pi(q)^\top \mathcal{G}(Q(\cdot)) \end{cases} \tag{13}$$

Let us consider $D = [I_m \vdots 0_{m\times(2n-m)}] \in \mathbb{R}^{m\times 2n}$. Replacing φ in (6), multiplying both sides of the first equation of (1) by $\Pi(q)^\top$, and using (13) one obtains the following Lagrangian system

$$\begin{cases} \mathbf{M}(\psi)\ddot\psi + \mathbf{C}(\psi,\dot\psi)\dot\psi + \mathbf{G}(\cdot;\psi) + \mathbb{K}(\cdot;\psi) = EU + D\lambda \\ 0 \leq \lambda \perp q_1 \geq 0, \\ \text{Collision rule} \end{cases} \tag{14}$$

since $\triangleq \Pi(q)^\top = E$, and the admissible domain $\Phi = \{\psi \mid D\psi \geq 0\}$[2]. The following result shows the role of the above changes of variables in our study of tracking control for the system (6).

Lemma 1 *Let* $(\varphi^\top, \dot{\varphi}^\top)^\top \in \mathbb{R}^{2n\times 2}$ *and* $(\psi^\top, \dot{\psi}^\top)^\top \in \mathbb{R}^{2n\times 2}$ *be the state trajectories of the systems* (6) *and* (14)*, respectively. Moreover, let* $(\varphi_d, \dot{\varphi}_d)$ *and* $(\psi_d, \dot{\psi}_d)$ *be the corresponding desired trajectories, where we set* $\varphi_d = Q(\psi_d)$, $\tilde{\varphi} = \varphi - \varphi_d$ *and* $\tilde{\psi} = \psi - \psi_d$. *Then*

$$\begin{pmatrix} \tilde{\varphi}(t) \\ \dot{\tilde{\varphi}}(t) \end{pmatrix} \underset{t\to+\infty}{\longrightarrow} 0 \quad \Longleftrightarrow \quad \begin{pmatrix} \tilde{\psi}(t) \\ \dot{\tilde{\psi}}(t) \end{pmatrix} \underset{t\to+\infty}{\longrightarrow} 0$$

Proof: First one assumes that ξ is of class $\mathcal{C}^1$. Therefore $x \mapsto \frac{d\xi}{d\varphi}(x)$ is continuous and it is bounded on compact sets. Consequently, for every segments $[a,b]$ in an open set of $\mathbb{R}^{n-m}$ we have

$$\|\xi(a) - \xi(b)\| \leq M\|a-b\|,$$

where $\|\frac{d\xi}{d\varphi}(x)\| \leq M$ for any $x \in [a,b]$. Since $\varphi = Q(\psi)$ one has

$$\begin{aligned} \varphi_{11} = \psi_{11} + \xi(\psi_{12}), \quad (\varphi_d)_{11} = (\psi_d)_{11} + \xi((\psi_d)_{12}), \\ \varphi_{12} = \psi_{12}, \quad \varphi_2 = \psi_2, \quad (\varphi_d)_{12} = (\psi_d)_{12}, \quad (\varphi_d)_2 = (\psi_d)_2. \end{aligned} \tag{15}$$

Using (15) one gets

$$\|\tilde{\varphi}_{11}(t)\| \leq (1+M)\|\tilde{\psi}_{11}(t)\|.$$

Clearly, if $\tilde{\psi}(t) \to 0$ as $t \to +\infty$ then $\tilde{\varphi}(t) \to 0$ as $t \to +\infty$. On the other hand, we have

$$\dot{\tilde{\varphi}}_{11}(t) = (I + \frac{d\xi}{d\varphi}(\psi_{12}(t))\dot{\tilde{\psi}}_{11}(t) + \left[\frac{d\xi}{d\varphi}(\psi_{12}(t)) - \frac{d\xi}{d\varphi}((\psi_d)_{12}(t))\right](\dot{\psi}_d)_{12}(t)$$

Thus, the continuity of $\frac{d\xi}{d\varphi}(\cdot)$ implies that $\dot{\tilde{\varphi}}(t) \underset{t\to+\infty}{\longrightarrow} 0$ when $\dot{\tilde{\psi}}(t) \underset{t\to+\infty}{\longrightarrow} 0$. The rest of the proof follows by the same arguments as above.

According to Lemma 1, we only focus our attention to tracking control for the transformed system (14).

It is noteworthy that applying the change of coordinates (12) the stiffness term $\mathbb{K}(\cdot;\psi)$ becomes nonlinear. In order to simplify the presentation we decompose $\mathbb{K}(\cdot;\psi)$ as the sum of a linear and a nonlinear term. First, let us define

$$\left\{ \begin{array}{l} P_1(\cdot;\psi) \triangleq K\left[\mathcal{Z}(\cdot) + \Pi'(q)(Q_1(\cdot) - Q_2(\cdot))\right] \\ P_2(\cdot;\psi) \triangleq -K\mathcal{Z}(\cdot) \end{array} \right. \tag{16}$$

where

[2] In particular it is implicitly assumed that the function $F_i(\cdot)$ in (1) are linearly independent.

$$\mathcal{Z}(\psi) \triangleq (\xi(q_2)^\top, 0_{n-m})^\top \quad \Pi'(q) \triangleq \begin{pmatrix} 0_{m\times m} & 0_{m\times(n-m)} \\ [\frac{\partial \xi}{\partial q_2}(q_2)]^\top & 0_{(n-m)\times(n-m)} \end{pmatrix} \in \mathbb{R}^{n\times n}$$

The following result gives the decomposition of the stiffness term $\mathbb{K}$ in (13) and it is obtained by straightforward arguments.

Lemma 2 *The nonlinear stiffness term $\mathbb{K}$ can be decomposed as*

$$\mathbb{K}(\cdot;\psi) = \mathcal{K}\cdot + P(\cdot;\psi). \tag{17}$$

where the matrix $\mathcal{K} = \begin{pmatrix} K & -K \\ -K & K \end{pmatrix}$ and $P(\cdot;\psi) = \left(P_1(\cdot;\psi)^\top, P_2(\cdot;\psi)^\top\right)^\top$ with $P_1(\cdot;\psi),\ P_2(\cdot;\psi)$ as in (16).

Furthermore, exploiting Lemma 2, definitions (13) and the particular form of $\mathcal{M}(\varphi)$, $\mathcal{C}(\varphi,\dot\varphi)$, $\mathcal{G}(\varphi)$ and $\Pi(q)$, the system (14) rewrites as

$$\left\{\begin{array}{l} M(q)\ddot q + C(q,\dot q)\dot q + G(q) + K(q-\theta) = D^\top\lambda \\ J\ddot\theta + K(\theta - q) - K\mathcal{Z}(\psi) = U \\ q_1 \geq 0,\ q_1\lambda = 0,\ \lambda \geq 0 \\ \text{Collision rule} \end{array}\right. \tag{18}$$

where $G(q) \in \mathbb{R}^n$ stands for the first n components of $\mathbf{G}(\psi;\psi) + P(\psi;\psi)$ (it is clear that $P_1(\psi,\psi)$ and the first n components of $\mathbf{G}(\psi;\psi)$ depends only on q) and

$$\left\{\begin{array}{l} M(q) = (I_n + \Pi'(q))M(X)(I_n + \Pi'(q))^\top \\ C(q,\dot q) = (I_n + \Pi'(q))C(X,\dot X)\left[(I_n + \Pi'(q))^\top + \frac{d}{dt}(I_n + \Pi'(q))^\top\right] \end{array}\right.$$

4 Tracking control framework

Throughout the paper, the following trajectories will play a role in the closed-loop dynamics:

- $X^{\text{nc}}(\cdot)$ denotes the desired trajectory that the system should track if there were no constraints. We suppose that $F(X^{\text{nc}}(t)) < 0$ for some t, otherwise the problem reduces to the tracking control of a system with no constraints.
- $X_d^*(\cdot)$ denotes the signal entering the control input and playing the role of the desired trajectory during some parts of the motion.
- $X_d(\cdot)$ represents the signal entering the Lyapunov function $V(\cdot)$. This signal is set on the boundary $\partial\Phi$ after the first impact of each cycle.

These signals may coincide on some time intervals as we shall see later.

Remark 2 *After the change of coordinates the above signals are denoted by $q^{nc}(\cdot),\ q_d^*(\cdot)$ and $q_d(\cdot)$ respectively. In case of free motion all three trajectories are the same "desired" trajectory.*

Let us remind that $\tilde\psi = \begin{pmatrix} \tilde q \\ \tilde\theta \end{pmatrix} = \psi - \psi_d$ and introduce the notations: $s_1 = \dot{\tilde q} + \gamma_2\tilde q,\ s_2 = \dot{\tilde\theta} + \gamma_2\tilde\theta,\ s = \begin{pmatrix} s_1 \\ s_2 \end{pmatrix}$, $\dot q_r = \dot q_d - \gamma_2\tilde q,\ \overline{q} = q - q_d^*$ and $\overline{s}_1 = \dot{\overline{q}} + \gamma_2\overline{q}$ where $\gamma_2 > 0$ is a scalar gain and $\psi_d = \begin{pmatrix} q_d \\ \theta_d \end{pmatrix}$ represents the desired trajectory.

4.1 Controller design

The tracking problem is solved using a generalization of the controller proposed in [13, Equ. (28)] and the closed-loop stability analysis of the system is based on Proposition 2. The controller is defined by

$$\begin{cases} U = J\ddot{\theta}_r + K(\theta_d - q_d) - \gamma_1 s_2 - K\mathcal{Z}(\psi) \\ \theta_d = q_d + K^{-1}U_r \end{cases} \tag{19}$$

where U_r is given by:

$$U_r = \begin{cases} U_c^{\emptyset} \triangleq U_{nc} = M(q)\ddot{q}_r + C(q,\dot{q})\dot{q}_r + G(q) - \gamma_1 s_1, \text{ for } t \in \Omega_{2k}^{\emptyset} \\ U_c^{B_k} = U_{nc} - P_d + K_f(P_q - P_d), \text{ for } t \in \Omega_k^{B_k} \\ U_c^{B_k}, \text{ for } t \in I_k^{B_k} \text{ before the first impact} \\ U_t^{B_k} = M(q)\ddot{q}_r + C(q,\dot{q})\dot{q}_r + G(q) - \gamma_1 \overline{s}_1, \text{ for } t \in I_k^{B_k} \text{ after the first impact} \end{cases} \tag{20}$$

where $\gamma_1 > 0$ is a scalar gain, $K_f > 0$, $P_q = D^T\lambda$ and $P_d = D^T\lambda_d$ is the desired contact force during the persistently constrained motion. It is clear that during $\Omega_k^{B_k}$ not all the constraints are active and, therefore, some components of λ and λ_d are zero. Notice that on impacting phases no force feedback is applied. Also U is a function of q, θ, $\dot{q}$, $\dot{\theta}$ only (no acceleration feedback).

The closed-loop error dynamics on $\Omega_{2k}^{\emptyset}$ (free-motion mode) is given by:

$$\begin{cases} M(q)\dot{s}_1 + C(q,\dot{q})s_1 + \gamma_1 s_1 + K(\tilde{q} - \tilde{\theta}) = 0 \\ J\dot{s}_2 + \gamma_1 s_2 + K(\tilde{\theta} - \tilde{q}) = 0 \end{cases}$$

The rationale behind the change of structure of U_r after the first impact, is that it facilitates the calculation of some upper-bounds which are necessary to recast the closed-loop stability analysis into Proposition 2 (see section 7).

In order to prove the stability of the closed-loop system (18)-(20) we will use the following positive definite function:

$$V(t,s,\tilde{\psi}) = \frac{1}{2}s_1^T M(q)s_1 + \frac{1}{2}s_2^T J s_2 + \gamma_1\gamma_2\tilde{q}^T\tilde{q} + \gamma_1\gamma_2\tilde{\theta}^T\tilde{\theta} + \frac{1}{2}(\tilde{q}-\tilde{\theta})^T K(\tilde{q}-\tilde{\theta}) \tag{21}$$

One of the difficulty of the flexible-joint case, compared with the rigid case, is that the jumps in the function $V(\cdot)$ in (21) are less easy to characterize. Indeed the terms $\theta_d(\cdot)$ and $\dot{\theta}_d(\cdot)$ are designed from a backstepping procedure and cannot be given arbitrary values, contrarily to the usual exogenous desired trajectories. The calculations of various upper-bounds (see the Section 7) are consequently intricate.

4.2 Design of the exogenous trajectories

We consider that the unconstrained desired trajectory $q^{\mathrm{nc}}(\cdot)$ can be split into two parts, one of them belonging to the admissible domain (inner part) and the other one outside the admissible domain (outer part). Throughout the paper we consider $I_k^{B_k} = [\tau_0^k, t_f^k]$ where τ_0^k is chosen by the designer as the start of the transition phase $I_k^{B_k}$, and t_f^k is the end of this phase. During the transition phases the system must be stabilized on the intersection of some surfaces Σ_i. This will be done by mimicking the behavior of a ball falling on the ground under gravity. Therefore all the components except the ones that are normal to the constraints belonging to B_k will be frozen. Moreover for robustness reasons one avoids a tangential approach and imposes some impacts defining a desired signal q_d^* that violates the constraints. In the sequel we deal with the tracking control strategy when the trajectory $q_d(\cdot)$ is constructed such that:

(i) when no activated constraint the orbit of $q_d(\cdot)$ coincides with the orbit of $q^{\text{nc}}(\cdot)$ and $\dot{q}_d(\tau_0^k) = 0$,

(ii) when $p \leq m$ constraints are active, its orbit coincides with the projection of the outer part of $q^{\text{nc}}(\cdot)$ on the surface of codimension p defined by the activated constraints (X_d between A'' and C in Figure 1),

In order to simplify the presentation we introduce the following notations (where all superscripts $(\cdot)^k$ will refer to the cycle k of the system motion):

- t_0^k is the first impact during the cycle k,
- t_∞^k is the accumulation point of the sequence $\{t_\ell^k\}_{\ell \geq 0}$ of the impact instants during the cycle k ($t_f^k \geq t_\infty^k$),
- τ_1^k will be explicitly defined later and represents the instant when the desired signal q_d^* reaches a given value chosen by the designer in order to impose a closed-loop dynamics with impacts during the transition phases,
- t_d^k is the desired detachment instant.

It is noteworthy that t_0^k, t_∞^k, t_d^k are state-dependent whereas τ_1^k and τ_0^k are exogenous and imposed by the designer. To better understand the definition of these specific instants, in Figure 1 we simplify the system's motion as follows:

- during transition phases we take into account only the constraints that must be activated $B'_k \setminus B_k$.
- at the end of $\Omega_{2k+1}^{B'_k}$-phases we take into account only the constraints that must be deactivated $B'_k \setminus B_{k+1}$.

The points A, A', A'' and C in Figure 1 correspond to the moments τ_0^k, t_0^k, t_f^k and t_d^k respectively. We have seen that the choice of τ_0^k plays an important role in the stability criterion given by Proposition 2. On the other hand in Figure 1 we see that starting from A the desired trajectory $X_d(\cdot) = X_d^*(\cdot)$ is deformed compared to $X^{\text{nc}}(\cdot)$. In order to reduce this deformation τ_0^k and implicitly the point A must be close to $\partial\Phi$. Further details on the choice of τ_0^k will be given later.

4.3 Design of $q_d^*(\cdot)$ and $q_d(\cdot)$ during the phases $I_k^{B_k}$

During the impacting transition phases the system must be stabilized on $\partial\Phi$. Obviously, this does not mean that all the constraints have to be activated (i.e. $q_1^i(t) = 0, \forall i = 1, \dots, m$). Let us consider that only the first p constraints (eventually reordering the coordinates) define the border of Φ where the system must be stabilized. On $[\tau_0^k, t_0^k)$ we define $q_d^*(\cdot)$ as a twice differentiable signal such that $q_d^*(\cdot)$ approaches a given point in the normal cone $N_\Phi(q_p = 0)$ on $[\tau_0^k, \tau_1^k]$. Precisely, τ_1^k is imposed by the designer

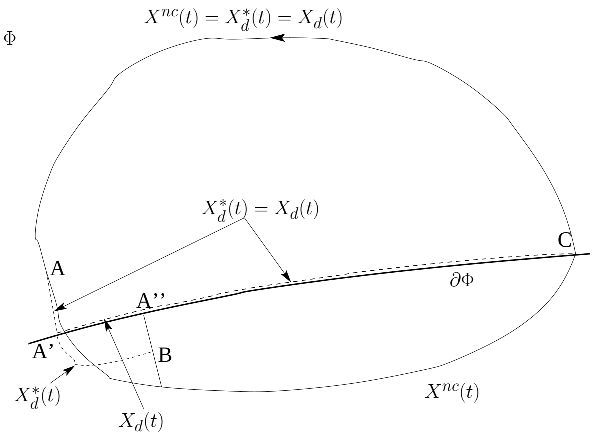

Figure 1: The closed-loop desired trajectory and control signals

as the instant where $(q_d^*)(\tau_1^k) = -\nu V^{1/3}(\tau_0^k) \times \underbrace{(1,\dots,1)}_{p}$. In other words, the choice of τ_1^k allows the definition of $q_d^*(\cdot)$ as a polynomial with limit conditions (see (22) and (23) below).

In order to facilitate the computation of some upper-bounds in Section 7 we explicitly define $q_d^*(\cdot)$ as follows:

- choosing $\nu > 0$ and denoting $t' = \frac{t-\tau_0^k}{\tau_1^k-\tau_0^k}$, the components $\left(q_d^i\right)^*$, $i = 1,\dots,p$ of $(q_d^*)_p$ are defined as:

$$\left(q_d^i\right)^*(t) = \begin{cases} a_3(t')^3 + a_2(t')^2 + a_0, & t \in [\tau_0^k, \min\{\tau_1^k; t_0^k\}] \\ -\nu V^{1/3}(\tau_0^k), & t \in (\min\{\tau_1^k; t_0^k\}, t_f^k] \end{cases} \tag{22}$$

  where $V(\cdot)$ is defined in (21) and with the coefficients given by:

$$\begin{aligned} a_3 &= 2[\left(q^i\right)^{\text{nc}}(\tau_0^k) + \nu V^{1/3}(\tau_0^k)] \\ a_2 &= -3[\left(q^i\right)^{\text{nc}}(\tau_0^k) + \nu V^{1/3}(\tau_0^k)] \\ a_0 &= \left(q^i\right)^{\text{nc}}(\tau_0^k) \end{aligned} \tag{23}$$

- all the other components of $q_d^*(\cdot)$ are frozen:

$$(q_d^*)_{n-p}(t) = q_{n-p}^{\text{nc}}(\tau_0^k), \quad t \in (\tau_0^k, t_f^k] \tag{24}$$

As we said before, the choice of $q_d^*(\cdot)$ is motivated by the robustness of the stabilization on $\partial\Phi$ by mimicking the bouncing-ball dynamics. On the other hand this enables one to compute suitable upper-bounds that will help using Proposition 2. The form of $q_d^*(\cdot)$ in (22) involves $-\nu V^{1/3}$ which is motivated by the fact that

- when the tracking error is not null, $q_d^*(\cdot)$ has to violate the constraint in order to assure the stabilization on it,

- some upper bounds of the jumps in $V(\cdot)$ are facilitated by such design and they tends to zero when the tracking error approaches zero.

In order to limit the deformation of the desired trajectory $q_d^*(\cdot)$ w.r.t. $q^{\text{nc}}(\cdot)$ during the I_k phases (see Figure 1), we impose in the sequel

$$||q_p^{\text{nc}}(\tau_0^k)|| \leq \nu_1 \tag{25}$$

where $\nu_1 > 0$ is chosen by the designer. It is obvious that a smaller ν_1 leads to a smaller deformation of the desired trajectory and to a smaller deformation of the real trajectory as we shall see in Section 8. Nevertheless, due to the tracking error, ν_1 cannot be chosen zero. We also note that (25) is a practical way to choose τ_0^k.

During the transition phases I_k we define $(q_d)_{n-p}(t) = (q_d^*)_{n-p}(t)$. Assuming a finite accumulation period, the impact process can be considered in some way equivalent to a plastic impact. Therefore, $(q_d)_p(\cdot)$ and $(\dot{q}_d)_p(\cdot)$ are set to zero on the right of t_0^k. On the left of t_0^k one has $(q_d)_p(\cdot) = (q_d^*)_p(\cdot)$ see Figure 3 for an example, see also Figure 1. It is worth to recall that the first impact time t_0^k of each cycle k, is unknown.

5 Design of the desired contact force during constraint phases

The desired contact force $P_d = D^\top \lambda_d$ must be designed such that it is large enough to assure the constraint motion on the $\Omega_{2k+1}^{B_k}$-phases. Some contact force components have also to be decreased at the end of the $\Omega_{2k+1}^{B_k}$-phases in order to allow the detachment. Therefore we need a lower bound of the desired force which assures both the contact (without any undesired detachment which can generate other impacts) during the $\Omega_{2k+1}^{B_k}$ phases and a smooth detachment at the end of $\Omega_{2k+1}^{B_k}$. Dropping the time argument, the dynamics of the system on $\Omega_{2k+1}^{B_k}$ can be written as

$$\begin{cases} M(q)\ddot{q} + F = (1+K_f)D_p^\top(\lambda - \lambda_d) \\ J\dot{s}_2 + \gamma_1 s_2 + K(\tilde{\theta} - \tilde{q}) = 0 \\ 0 \leq q_p \perp \lambda_p \geq 0 \end{cases} \tag{26}$$

where $F = F(q, \dot{q}, \tilde{q}, \dot{\tilde{q}}, \tilde{\theta}) = -M(q)\ddot{q}_r + C(q,\dot{q})s_1 + \gamma_1 s_1 + K(\tilde{q} - \tilde{\theta})$ and $D_p = [I_p \vdots O_{p\times(n-p)}] \in \mathbb{R}^{p\times n}$. On $\Omega_{2k+1}^{B_k}$ the system has to be permanently constrained which is equivalent to $q_p(\cdot) = 0$ and $\dot{q}_p(\cdot) = 0$. In order to assure these conditions it is sufficient to have $\lambda_p > 0$.

In the following let us denote $M^{-1}(q) = \begin{pmatrix} [M^{-1}(q)]_{p,p} & [M^{-1}(q)]_{p,n-p} \\ [M^{-1}(q)]_{n-p,p} & [M^{-1}(q)]_{n-p,n-p} \end{pmatrix}$ and
$C(q,\dot{q}) = \begin{pmatrix} C(q,\dot{q})_{p,p} & C(q,\dot{q})_{p,n-p} \\ C(q,\dot{q})_{n-p,p} & C(q,\dot{q})_{n-p,n-p} \end{pmatrix}$ where the meaning of each component is obvious. Let us also denote by K_p the matrix made of the first p rows and p columns of K.

Proposition 3 *On $\Omega_k^{B_k}$ the constraint motion of the closed-loop system (26) (19) (20) is assured if the desired contact force is defined by*

$$
\begin{aligned}
(\lambda_d)_p \triangleq \nu_p + \frac{K_p\tilde{\theta}_p}{1+K_f} - \frac{\bar{M}_{p,p}(q)}{1+K_f}\Big([M^{-1}(q)]_{p,p}C_{p,n-p}(q,\dot{q}) \\
+ [M^{-1}(q)]_{p,n-p}C_{n-p,n-p}(q,\dot{q}) + \gamma_1[M^{-1}(q)]_{p,n-p}\Big)(s_1)_{n-p}
\end{aligned}
\tag{27}
$$

where $\bar{M}_{p,p}(q) = \big([M^{-1}(q)]_{p,p}\big)^{-1} = \big(D_pM^{-1}(q)D_p^T\big)^{-1}$ is the inverse of the so-called Delassus' matrix [30] and $\nu_p \in \mathbb{R}^p$, $\nu_p > 0$.

Proof: It is noteworthy that the third relation in (26) implies on $\Omega_{2k+1}^{B_k}$ (see [18])

$$
0 \le \ddot{q}_p \perp \lambda_p \ge 0 \Leftrightarrow 0 \le D_p\ddot{q} \perp \lambda_p \ge 0. \tag{28}
$$

From (26) one easily gets:

$$
\ddot{q} = M^{-1}(q)\big[-F + (1+K_f)D_p^\top(\lambda-\lambda_d)_p\big]
$$

Combining the last two equations we obtain the following LCP with unknown λ:

$$
0 \le D_pM^{-1}(q)\big[-F-(1+K_f)D_p^\top(\lambda_d)_p\big] + (1+K_f)D_pM^{-1}(q)D_p^\top\lambda_p \perp \lambda_p \ge 0 \tag{29}
$$

Since $(1+K_f)D_pM^{-1}(q)D_p^\top > 0$ and hence is a P-matrix, the LCP (29) has a unique solution and one deduces that $\lambda_p > 0$ if and only if

$$
\begin{aligned}
&\frac{\bar{M}_{p,p}(q)}{1+K_f}D_pM^{-1}(q)\big[-F-(1+K_f)D_p^T(\lambda_d)_p\big] < 0 \Leftrightarrow \\
&(\lambda_d)_p > -\frac{\bar{M}_{p,p}(q)}{1+K_f}D_pM^{-1}(q)F \Leftarrow \\
&(\lambda_d)_p = \nu_p - \frac{\bar{M}_{p,p}(q)}{1+K_f}D_pM^{-1}(q)F
\end{aligned}
\tag{30}
$$

with $\nu_p \in \mathbb{R}^p$, $\nu_p > 0$. Since $F = -M(q)\ddot{q}_r + C(q,\dot{q})s_1 + \gamma_1 s_1 + K(\tilde{q} - \tilde{\theta})$, $(\ddot{q}_r)_p = 0$ and $(s_1)_p = 0$, (30) rewrites as (27) and the proof is finished. It is noteworthy that the solution of the LCP (29) is

$$
\begin{aligned}
\lambda_p &= \frac{\bar{M}_{p,p}(q)}{1+K_f}D_pM^{-1}(q)\big[F + (1+K_f)D_p^\top(\lambda_d)_p\big] \\
&= (\lambda_d)_p + \frac{\bar{M}_{p,p}(q)}{1+K_f}D_pM^{-1}(q)F = \nu_p
\end{aligned}
\tag{31}
$$

where (27) has been used.

6 Strategy for take-off at the end of constraint phases $\Omega_{2k+1}^{B_k}$

In this Section we are interested in finding the conditions on the control signal $U_c^{B_k}$ that assures the take-off at the end of constraint phases $\Omega_{2k+1}^{B_k}$. As we have already seen before, the phase $\Omega_{2k+1}^{B_k}$ corresponds to the time interval $[t_f^k, t_d^k)$. The dynamics on $[t_f^k, t_d^k)$ is given by (26) and the system is permanently constrained, which implies $q_p(\cdot) = 0$ and $\dot{q_p}(\cdot) = 0$. Let us also consider that the first h constraints ($h < p$) have to be deactivated. Thus, the detachment takes place at t_d^k if $\ddot{q}_h(t_d^{k+}) > 0$ which requires $\lambda_h(t_d^{k-}) = 0$. The last $p-h$ constraints remain active which means $\lambda_{p-h}(t_d^{k-}) > 0$.

To simplify the notation we drop the time argument in many equations of this section. We decompose the LCP matrix (which is the Delassus' matrix multiplied by $1 + K_f$) as:

$$(1+K_f)D_pM^{-1}(q)D_p^T = \begin{pmatrix} A_1(q) & A_2(q) \\ A_2(q)^T & A_3(q) \end{pmatrix} \tag{32}$$

with $A_1 \in \mathbb{R}^{h\times h}$, $A_2 \in \mathbb{R}^{h\times(p-h)}$ and $A_3 \in \mathbb{R}^{(p-h)\times(p-h)}$

Proposition 4 *The closed-loop system (26) (19) (20) is permanently constrained on* $[t_f^k, t_d^k)$ *and a smooth detachment is guaranteed on* $[t_d^k, t_d^k + \epsilon)$ *(*ϵ *is a small positive real number chosen by the designer) if*

(i)

$$\begin{pmatrix} (\lambda_d)_h\,(t_d^k) \\ (\lambda_d)_{p-h}\,(t_d^k) \end{pmatrix} = \begin{pmatrix} \left(A_1 - A_2A_3^{-1}A_2^T\right)^{-1}\left(b_h - A_2A_3^{-1}b_{p-h}\right) - C_1(t-t_d^k) \\ C_2 + A_3^{-1}\left(b_{p-h} - A_2^T\,(\lambda_d)_h\right) \end{pmatrix} \tag{33}$$

where

$$b_p = b_p(q,\dot{q},U_c^{\emptyset}) \triangleq -D_pM^{-1}(q)F \geq 0$$

and $C_1 \in \mathbb{R}^h$, $C_2 \in \mathbb{R}^{p-h}$ *such that* $C_1 \geq 0$, $C_2 > 0$.

(ii) *On* $[t_d^k, t_d^k + \epsilon)$

$$q_d^*(t) = q_d(t) = \begin{pmatrix} q_h^*(t) \\ q_{n-h}^{nc}(t) \end{pmatrix},$$

where $q_h^*(\cdot)$ *is a twice-differentiable function such that*

$$\begin{aligned} q_h^*(t_d^k) = 0, \quad q_h^*(t_d^k+\epsilon) = q_h^{nc}(t_d^k+\epsilon), \\ \dot{q}_h^*(t_d^k) = 0, \quad \dot{q}_h^*(t_d^k+\epsilon) = \dot{q}_h^{nc}(t_d^k+\epsilon) \end{aligned} \tag{34}$$

and $\ddot{q}_h^*(t_d^{k+}) = a > \max\left(0, -A_1(q)(\lambda_d)_h(t_d^{k-})\right)$.

Proof: The necessary condition for take-off after the instant t_d^k is given by $\lambda_h(t_d^{k-}) = 0$ and $\lambda_{p-h}(t_d^{k-}) > 0$. Precisely, we impose a positive contact force on $[t_f^k, t_d^k)$ with the first h components approaching 0 when t approaches t_d^k. From (32) and (26) it is straightforward that the LCP (28) rewrites as:

$$0 \leq \begin{pmatrix} \lambda_h \\ \lambda_{p-h} \end{pmatrix} \perp \begin{pmatrix} b_h + A_1(\lambda - \lambda_d)_h + A_2(\lambda - \lambda_d)_{p-h} \\ b_{p-h} + A_2^T(\lambda - \lambda_d)_h + A_3(\lambda - \lambda_d)_{p-h} \end{pmatrix} \geq 0 \qquad (35)$$

Since $(1 + K_f)D_p M^{-1}(q) D_p^T > 0$, the LCP (28) (or the equivalent one (35)) has a unique solution. Imposing $\lambda_h = 0$ one gets

$$0 \leq \lambda_{p-h} \perp b_{p-h} - A_2^T(\lambda_d)_r + A_3(\lambda - \lambda_d)_{p-h} \geq 0$$

with the solution

$$\lambda_{p-h} = -A_3^{-1}\left(b_{p-h} - A_2^T(\lambda_d)_h - A_3(\lambda_d)_{p-h}\right) \qquad (36)$$

Thus $\lambda_{p-h} > 0$ is equivalent to

$$(\lambda_d)_{p-h} > A_3^{-1}\left(b_{p-h} - A_2^T\,(\lambda_d)_h\right)$$

which leads to the second part of definition (33). Furthermore, replacing $(\lambda_d)_{p-h}$ in (36) we get $\lambda_{p-h} = C_2$ and $b_h + A_1(\lambda - \lambda_d)_h + A_2(\lambda - \lambda_d)_{p-h} \geq 0$ yields the first part of definition (33). Consequently the solution of the LCP (35) is $\lambda_p = \begin{pmatrix} 0 \\ C_2 \end{pmatrix} \in \mathbb{R}^p$ when $(\lambda_d)_p$ is defined by (33).

The jumps in the Lyapunov function are avoided during the detachment phase using a twice differentiable desired trajectory $q_d(\cdot)$ defined as in item **(ii)** of the Proposition. In order to assure a smooth detachment (without impacts) on $[t_d^k, t_d^k + \epsilon)$ we need a large enough positive desired acceleration $(\ddot{q}_d)_h$. At t_d^{k-} one has

$$\ddot{q}_h(t_d^{k-}) = -D_h M^{-1}(q)\left[F + (1 + K_f)D_h^\top(\lambda_d)_h\right]$$

while at t_d^{k+} one has $\ddot{q}_{p-h}(t_d^{k+}) = D_h M^{-1}(q) F$. Since $(\ddot{q}_d)_h(t_d^{k-}) = 0$ we arrive at

$$\sigma_{\ddot{q}_h(t_d^k)} = (\ddot{q}_d)_h(t_d^{k+}) + A_1(q)(\lambda_d)_h(t_d^{k-})$$

Therefore $\ddot{q}_{1d}(t_d^{k+})$ has to be positive and large enough in order to compensate for $-A_1(q)(\lambda_d)_h(t_d^{k-})$ at the instant t_d^k. Consequently one defines

$$\ddot{q}_1^*(t_d^{k+}) = a > \max\left(0, -A_1(q)(\lambda_d)_h(t_d^{k-})\right)$$

and the detachment is assured.

7 Closed-loop stability analysis

To simplify the notation $V(t, s(t), \tilde{\psi}(t))$ is denoted as $V(t)$. In order to introduce the main result of this paper we make the next assumption, which is verified in practice for dissipative systems with $e \in [0, 1)$ (see numerical experiments in Section 8).

Assumption 1 *The controller U in (19) (20) assures that all the transition phases are finite.*

Lemma 3 *Consider the closed-loop system (18)-(20) with $(q_d^*)_p(\cdot)$ defined on the interval $[\tau_0^k, t_0^k]$ as in (22)-(24). Let us also suppose that condition* **b)** *of Proposition 2 is satisfied. The following inequalities hold:*

$$
\begin{aligned}
&||\tilde{q}(t_0^{k-})|| \leq \sqrt{\frac{V(\tau_0^k)}{\gamma_1\gamma_2}}, \quad ||s_1(t_0^{k-})|| \leq \sqrt{\frac{2V(\tau_0^k)}{\lambda_{min}(M(q))}},\\
&||\tilde{\theta}(t_0^{k-})|| \leq \sqrt{\frac{V(\tau_0^k)}{\gamma_1\gamma_2}}, \quad ||s_2(t_0^{k-})|| \leq \sqrt{\frac{2V(\tau_0^k)}{\lambda_{min}(J)}},
\end{aligned} \tag{37}
$$

and

$$
\begin{aligned}
||\dot{\tilde{q}}(t_0^{k-})|| &\leq \left(\sqrt{\frac{2}{\lambda_{min}(M(q))}} + \sqrt{\frac{\gamma_2}{\gamma_1}}\right) V^{1/2}(\tau_0^k)\\
||\dot{\tilde{\theta}}(t_0^{k-})|| &\leq \left(\sqrt{\frac{2}{\lambda_{min}(J)}} + \sqrt{\frac{\gamma_2}{\gamma_1}}\right) V^{1/2}(\tau_0^k)
\end{aligned} \tag{38}
$$

Furthermore, if $t_0^k \leq \tau_1^k$ one has

$$
\begin{aligned}
&||(q_d)_p(t_0^{k-})|| \leq \epsilon + \sqrt{\frac{V(\tau_0^k)}{\gamma_1\gamma_2}}, \quad ||(\dot{q}_d)_p(t_0^{k-})|| \leq \bar{k} + k^* V^{1/6}(\tau_0^k)\\
&||(\ddot{q}_d)_p(t_0^{k-})||,\ ||(q_d^{(3)})_p(t_0^{k-})|| \leq 6\sqrt{2}\big(||q_p^{nc}(\tau_0^k)|| + \sqrt{p}\nu V^{1/2}(\tau_0^k)\big)
\end{aligned} \tag{39}
$$

where ϵ is the real constant fixed in Definition 3 and $\bar{k},\ k^* > 0$ are some constant real numbers that will be defined in the proof.

Proof: From (21) we can deduce that

$$
V(t_0^{k-}) \geq \gamma_1\gamma_2||\tilde{q}(t_0^{k-})||^2, \quad V(t_0^{k-}) \geq \frac{1}{2} s_1^\top(t_0^{k-}) M(q(t_0^{k-})) s_1(t_0^{k-})
$$

and

$$
V(t_0^{k-}) \geq \gamma_1\gamma_2||\tilde{\theta}(t_0^{k-})||^2, \quad V(t_0^{k-}) \geq \frac{1}{2} s_2^\top(t_0^{k-}) J s_2(t_0^{k-})
$$

Since condition **b)** of Proposition 2 is satisfied one has $V(\tau_0^k) \geq V(t_0^{k-})$ and (37) becomes trivial. Let us recall that $s_1(t) = \dot{\tilde{q}}(t) + \gamma_2\tilde{q}(t)$ and $s_2(t) = \dot{\tilde{\theta}}(t) + \gamma_2\tilde{\theta}(t)$ which implies $||\dot{\tilde{q}}(t_0^{k-})|| \leq ||s_1(t_0^{k-})|| + \gamma_2||\tilde{q}(t_0^{k-})||$ and $||\dot{\tilde{\theta}}(t_0^{k-})|| \leq ||s_2(t_0^{k-})|| + \gamma_2||\tilde{\theta}(t_0^{k-})||$ respectively. Combining this with (37) we derive (38).

The proof of (39) follows the ideas presented in [29]. Roughly the first inequality in (39) is based on the definition of p_ϵ-impacts (see Definition 3). The remaining inequalities in (39) are based on the particular definition of $(q_d^*)_p(\cdot)$ (see (22) (23)). Precisely, we recall that $t_0^k \leq \tau_1^k$ implies $(q_d)_p(t_0^{k-}) = (q_d^*)_p(t_0^k)$. It is clear that

$$||(q_d)_p(t_0^{k-})|| \leq ||\tilde{q}_p(t_0^{k-})|| + ||q_p(t_0^k)||$$

Taking into account that t_0^k is a p_ϵ-impact (which means $||q_p(t_0^k)|| \leq \epsilon$), the first inequality in (39) becomes obvious.

Let us denote $t'_k = \frac{t_0^k - \tau_0^k}{\tau_1^k - \tau_0^k} \in [0,1]$. We recall here that τ_0^k was chosen such that $||q_p^{\text{nc}}(\tau_0^k)|| \leq \nu_1$. From (22), (23) and the first inequality in (39), for $i = 1, \ldots, p$ one has

$$q_d^i(t_0^{k-}) = \left[(q^i)^{\text{nc}}(\tau_0^k) + \nu V^{1/3}(\tau_0^k)\right]\left(2(t'_k)^3 - 3(t'_k)^2\right) + (q^i)^{\text{nc}}(\tau_0^k) \leq \epsilon + \sqrt{\frac{V(\tau_0^k)}{\gamma_1\gamma_2}}$$

It follows that

$$3(t'_k)^2 - 2(t'_k)^3 \geq \frac{(q^i)^{\text{nc}}(\tau_0^k) - \epsilon - \sqrt{\frac{V(\tau_0^k)}{\gamma_1\gamma_2}}}{(q^i)^{\text{nc}}(\tau_0^k) + \nu V^{1/3}(\tau_0^k)}$$

For $t > 0$ one has $2t - t^2 \geq 3t^2 - 2t^3$, therefore

$$2t'_k - (t'_k)^2 \geq \frac{(q^i)^{\text{nc}}(\tau_0^k) - \epsilon - \sqrt{\frac{V(\tau_0^k)}{\gamma_1\gamma_2}}}{(q^i)^{\text{nc}}(\tau_0^k) + \nu V^{1/3}(\tau_0^k)}$$

which means that

$$\begin{aligned}(1 - t'_k)^2 &\leq 1 - \frac{(q^i)^{\text{nc}}(\tau_0^k) - \epsilon - \sqrt{\frac{V(\tau_0^k)}{\gamma_1\gamma_2}}}{(q^i)^{\text{nc}}(\tau_0^k) + \nu V^{1/3}(\tau_0^k)} \\ &= \frac{\sqrt{\frac{V(\tau_0^k)}{\gamma_1\gamma_2}} + \nu V^{1/3}(\tau_0^k) + \epsilon}{(q^i)^{\text{nc}}(\tau_0^k) + \nu V^{1/3}(\tau_0^k)}\end{aligned}$$

Straightforward computations lead to

$$|\dot{q}_d^i(t_0^{k-})| = \frac{6((q^i)^{\text{nc}}(\tau_0^k) + \nu V^{1/3}(\tau_0^k))}{\tau_1^k - \tau_0^k}\left(t'_k - (t'_k)^2\right)$$

Since $t'_k - (t'_k)^2 \leq 1 - t'_k$ and $(q^i)^{\text{nc}}(\tau_0^k) \leq \nu_1$, one arrives at

$$|\dot{q}_d^i(t_0^{k-})| \leq \frac{6\sqrt{\nu_1\epsilon}}{\tau_1^k - \tau_0^k} + \frac{6\sqrt{\left(\frac{1}{\sqrt{\gamma_1\gamma_2}} + \nu\right)(\nu + \nu_1) + \epsilon\nu}}{\tau_1^k - \tau_0^k} V^{1/6}(\tau_0^k) \tag{40}$$

Therefore, the second inequality in (39) holds with

$$\bar{k} = \frac{6\sqrt{p\nu_1\epsilon}}{\tau_1^k - \tau_0^k}, \quad k^* = \frac{6\sqrt{p}}{\tau_1^k - \tau_0^k}\sqrt{\left(\frac{1}{\sqrt{\gamma_1\gamma_2}} + \nu\right)(\nu + \nu_1) + \epsilon\nu}$$

Finally, differentiating (22) two and three times respectively one obtains

$$\begin{aligned}
\ddot{q}_d^i(t_0^{k-}) &= \lim_{t\to t_0^k, t<t_0^k} 6((q^i)^{\text{nc}}(\tau_0^k)+\nu V^{1/2}(\tau_0^k))(2t'-1)\\
&\le \lim_{t\to t_0^k, t<t_0^k} 6((q^i)^{\text{nc}}(\tau_0^k)+\nu V^{1/2}(\tau_0^k))\\
(q_d^i)^{(3)}(t_0^{k-}) &= \lim_{t\to t_0^k, t<t_0^k} 6((q^i)^{\text{nc}}(\tau_0^k)+\nu V^{1/2}(\tau_0^k))
\end{aligned}$$

which leads to the upper bounds of $||(\ddot{q}_d)_p(t_0^{k-})||$ and $||(q_d^{(3)})_p(t_0^{k-})||$ respectively.

It is noteworthy that $q(\cdot)$ is a continuous signal. Nevertheless $\dot{q}(\cdot)$ presents discontinuities of the first kind at the impact times. From (20) one deduces that the controller U_r jumps also at the impact times generating a jump in the desired signal $\theta_d(\cdot)$. Therefore, in order to study the evolution of the Lyapunov function candidate (21) one has to analyze $\sigma_{\tilde{\theta}}(\cdot)$ and $\sigma_{\dot{\tilde{\theta}}}(\cdot)$.

Lemma 4 *The controller U in (19) (20) guarantees that* $||\sigma_{\tilde{\theta}}(\cdot)||,\ ||\sigma_{\dot{\tilde{\theta}}}(\cdot)|| \in S(1) \equiv L^\infty$.

Proof: Since $\theta(\cdot), \dot{\theta}(\cdot)$ are continuous on $\mathbb{R}_+$ and $\theta_d(\cdot), \dot{\theta}_d(\cdot)$ are continuous on $\mathbb{R}_+ \setminus \{t_0^k \mid k \in \mathbb{Z}\}$ one deduces that $\sigma_{\tilde{\theta}}(t) = 0 = \sigma_{\dot{\tilde{\theta}}}(t),\ \forall t \neq t_0^k$. Therefore Lemma 4 holds if there exist some real constants that upper-bound $||\sigma_{\tilde{\theta}}(t_0^k)||,\ ||\sigma_{\dot{\tilde{\theta}}}(t_0^k)||,\ \forall k \in \mathbb{Z}$. The definition of $\theta_d(\cdot)$ (see (19)) allows us to write

$$\begin{aligned}
\sigma_{\tilde{\theta}}(t_0^k) &= -\sigma_{\theta_d}(t_0^k) = -\sigma_{q_d}(t_0^k) - K^{-1}\sigma_{U_r}(t_0^k) = \begin{pmatrix} (q_d)_p(t_0^{k-}) \\ 0 \end{pmatrix} - K^{-1}\sigma_{U_r}(t_0^k)\\
\sigma_{\dot{\tilde{\theta}}}(t_0^k) &= -\sigma_{\dot{\theta}_d}(t_0^k) = -\sigma_{\dot{q}_d}(t_0^k) - K^{-1}\sigma_{\dot{U}_r}(t_0^k) = \begin{pmatrix} (\dot{q}_d)_p(t_0^{k-}) \\ 0 \end{pmatrix} - K^{-1}\sigma_{\dot{U}_r}(t_0^k)
\end{aligned} \tag{41}$$

Therefore

$$\begin{aligned}
||\sigma_{\tilde{\theta}}(t_0^k)|| &\le ||(q_d)_p(t_0^{k-})|| + \lambda_{max}(K^{-1})||\sigma_{U_r}(t_0^k)||\\
||\sigma_{\dot{\tilde{\theta}}}(t_0^k)|| &\le ||(\dot{q}_d)_p(t_0^{k-})|| + \lambda_{max}(K^{-1})||\sigma_{\dot{U}_r}(t_0^k)||
\end{aligned}$$

Using (20) one obtains

$$\sigma_{U_r}(t_0^k) = M(q)\sigma_{\ddot{q}_r}(t_0^k) + \sigma_{C(q,\dot{q})\dot{q}_r}(t_0^k) - \gamma_1\sigma_{s_1}(t_0^k)$$

From (24) one has $(\dot{q}_d)_{n-p}(t) = 0,\ (\ddot{q}_d)_{n-p}(t) = 0\ \forall t \in [\tau_0^k, t_f^k]$. Moreover, as we have mentioned at the end of Section 4, $(q_d)_p(\cdot),\ (\dot{q}_d)_p(\cdot)$ and implicitly $(\ddot{q}_d)_p(\cdot)$ are set to zero on $(t_0^k, t_f^k]$. Thus taking into account the relation $||\dot{q}(t_0^{k+})|| \le ||\dot{q}(t_0^{k-})||$ (see [23]), Property 10 and Definition 5 one arrives at

$$\begin{aligned}
&||\sigma_{\ddot{q}_r}(t_0^k)|| \le ||(\ddot{q}_d)_p(t_0^{k-})|| + \gamma_2||(\dot{q}_d)_p(t_0^{k-})|| + 2\gamma_2||\dot{q}(t_0^{k-})||\\
&||\sigma_{C(q,\dot{q})\dot{q}_r}(t_0^k)|| \le ||\sigma_{C(q,\dot{q})}\dot{q}_r(t_0^{k-})|| + ||C(q,\dot{q}(t_0^{k+}))\sigma_{\dot{q}_r}(t_0^k)||\\
&\in S\big(2(1+\gamma_2)||\dot{q}(t_0^{k-})||\cdot||(\dot{q}_d)_p(t_0^{k-})|| + \gamma_2||(q_d)_p(t_0^{k-})||\big)\\
&||\sigma_{s_1}(t_0^k)|| \le 2||\dot{q}(t_0^{k-})|| + ||(\dot{q}_d)_p(t_0^{k-})|| + \gamma_2||(q_d)_p(t_0^{k-})||
\end{aligned} \tag{42}$$

When $V(\tau_0^k) \leq 1$, Lemma 3 states that $||(\dot{q}_d)_p(t_0^{k-})||,\ ||(q_d)_p(t_0^{k-})||$ and $||\dot{q}(t_0^{k-})||$ are bounded by some constants. Thus all the quantities in (42) are bounded by some constants independent of the cycle index k. This means that $||\sigma_{U_r}(t_0^k)||$ is bounded by a constant independent of the cycle index which implies the same for $||\sigma_{\tilde{\theta}}(t_0^k)||$. In other words $||\sigma_{\tilde{\theta}}(t)|| \in S(1)$.

Differentiating (20) one obtains

$$\dot{U}_r(t) = M(q)q_r^{(3)}(t) + \dot{M}(q)\ddot{q}_r(t) + C(q,\dot{q})\ddot{q}_r(t) + \dot{C}(q,\dot{q})\dot{q}_r(t) + \frac{\partial G}{\partial q}\dot{q}(t) - \gamma_1 \dot{s}_1(t) \tag{43}$$

where $\dot{M}$, $\dot{C}$ stand for $\frac{dM}{dt}$ and $\frac{dC}{dt}$ respectively.
It is clear that

$$\dot{C}(q,\dot{q})(t) = \frac{\partial C}{\partial q}(q,\dot{q})\dot{q}(t) + \frac{\partial C}{\partial \dot{q}}(q,\dot{q})\ddot{q}(t)$$

and using Properties 1 and 3 one derives

$$||\dot{C}(q,\dot{q})(t)|| \in S(||\dot{q}(t)||^2 + ||\ddot{q}(t)||)$$

Furthermore, Lemma 3 and the first equation in (18) assure that $||\dot{q}(t)||^2, ||\ddot{q}(t)|| \in S(1)$. Thus $||\dot{C}(q,\dot{q})(\cdot)||,\ ||\sigma_{\dot{C}(q,\dot{q})}(\cdot)|| \in S(1)$ and one derives that

$$||\sigma_{\dot{C}(q,\dot{q})}(t_0^k)\dot{q}_r(t_0^k)|| \leq ||\sigma_{\dot{C}(q,\dot{q})}(t_0^k)||.||\dot{q}_r(t_0^{k+})|| + ||\dot{C}(q,\dot{q})(t_0^{k-})||.||\sigma_{\dot{q}_r}(t_0^k)|| \in S(1) \tag{44}$$

Property 1 allows us to replace $\dot{M}(q)$ by $C(q,\dot{q}) + C^\top(q,\dot{q})$ which leads to

$$\begin{aligned} &\dot{M}(q)\ddot{q}_r(t) + C(q,\dot{q})\ddot{q}_r(t) = (2C(q,\dot{q}) + C^\top(q,\dot{q}))\ddot{q}_r(t) \Rightarrow \\ &||\dot{M}(q)\ddot{q}_r(t) + C(q,\dot{q})\ddot{q}_r(t)|| \leq 3||C(q,\dot{q})||.||\ddot{q}_r(t)|| \in S(||\dot{q}||.||\ddot{q}_r(t))||) \end{aligned}$$

Since $||\ddot{q}_r(t))|| \leq ||\ddot{q}_d(t)|| + \gamma_2||\dot{\tilde{q}}(t)||$, using Lemma 3 one gets

$$||\dot{M}(q)\ddot{q}_r(t) + C(q,\dot{q})\ddot{q}_r(t)|| \in S(1) \tag{45}$$

The definitions (22)-(24) and the first equation in (18) assure that $||q_r^{(3)}(t)|| \in S(1)$. Therefore

$$||M(q)q_r^{(3)}(t)|| \leq \lambda_{max}(M)||q_r^{(3)}(t)|| \in S(1) \tag{46}$$

Property 2 states that $||\frac{\partial G}{\partial q}|| \in S(1)$, which implies

$$\left.\begin{array}{l} \left|\left|\frac{\partial G}{\partial q}\dot{q}(t)\right|\right| \in S(||\dot{q}(t)||) \\ ||\dot{q}(t)|| \in S(1) \end{array}\right\} \Rightarrow \left|\left|\frac{\partial G}{\partial q}\dot{q}(t)\right|\right| \in S(1) \tag{47}$$

Introducing (44)–(47) in (43) and taking into account the last inequality in (42) we arrive at $||\sigma_{\dot{U}_r}(t)|| \in S(1)$ and thus $||\sigma_{\dot{\tilde{\theta}}}(t)|| \in S(1)$.

We now state the main result of this paper.

Theorem 2 *Let Assumption 1 hold, $e = 0$ and $q_d^*(\cdot)$ defined as in (22)-(24). The closed-loop system (18)-(20) initialized on Ω_0 such that $V(\tau_0^0) \leq 1$, satisfies the requirements of Proposition 2 and is therefore practically weakly stable with the closed-loop state $x(\cdot) = [\tilde{\psi}(\cdot), s(\cdot)]$ and $R = \sqrt{e^{-\gamma(t_f^k - t_\infty^k)}(\rho^* + \xi)/\bar{\rho}}$ where ρ^*, $\bar{\rho}$ and ξ are defined in the proof.*

Proof: First we observe that conditions **a)** and **c)** of Proposition 2 hold when the hypothesis of the Theorem are verified. Thus Theorem 2 holds if the conditions **b)**, **d)** of Proposition 2 are verified.

b) Using that $\dot{M}(q) - 2C(q,\dot{q})$ is a skew-symmetric matrix (see Property 1), straightforward computations show that on $\mathbb{R}_+ \setminus \bigcup_{k \geq 0}[t_0^k, t_f^k]$ the time derivative of the Lyapunov function is given by

$$\begin{aligned}\dot{V}(t) &= -\gamma_1||\dot{\tilde{q}}||^2 - \gamma_1\gamma_2^2||\tilde{q}||^2 - \gamma_1||\dot{\tilde{\theta}}||^2 - \gamma_1\gamma_2^2||\tilde{\theta}||^2 - \gamma_2(\tilde{q} - \tilde{\theta})^\top K(\tilde{q} - \tilde{\theta}) \\ &\quad + (1 + K_f)s_1^\top D_p^\top(\lambda - \lambda_d)_p \\ &= -\gamma_1||\dot{\tilde{q}}||^2 - \gamma_1\gamma_2^2||\tilde{q}||^2 - \gamma_1||\dot{\tilde{\theta}}||^2 - \gamma_1\gamma_2^2||\tilde{\theta}||^2 - \gamma_2(\tilde{q} - \tilde{\theta})^\top K(\tilde{q} - \tilde{\theta}) \leq 0\end{aligned}$$

where we have used the fact that $(q_d)_p \equiv 0$, $(\dot{q}_d)_p \equiv 0, q_p \equiv 0$, $\dot{q}_p \equiv 0$ thus $(s_1)_p \equiv 0$ on constraint phases, and $\lambda_p \equiv 0$, $(\lambda_d)_p \equiv 0$ on free-motion phases. On the other hand

$$\begin{aligned}V(t) &\leq \frac{\lambda_{max}(M(q))}{2}||s_1||^2 + \frac{\lambda_{max}(J)}{2}||s_2||^2 + \gamma_1\gamma_2||\tilde{q}||^2 + \gamma_1\gamma_2||\tilde{\theta}||^2 \\ &\quad + \frac{1}{2}(\tilde{q} - \tilde{\theta})^\top K(\tilde{q} - \tilde{\theta}) \\ &\leq \gamma^{-1}[\gamma_1||\dot{\tilde{q}}||^2 + \gamma_1\gamma_2^2||\tilde{q}||^2 + \gamma_1||\dot{\tilde{\theta}}||^2 + \gamma_1\gamma_2^2||\tilde{\theta}||^2 + \gamma_2(\tilde{q} - \tilde{\theta})^\top K(\tilde{q} - \tilde{\theta})]\end{aligned}$$

where

$$\gamma^{-1} = \max\left\{\lambda_{max}(\mathbf{M}(\psi))\frac{1 + 2\gamma_2}{2\gamma_1}; \frac{\lambda_{max}(\mathbf{M}(\psi))(\gamma_2 + 2) + 2\gamma_1}{2\gamma_1\gamma_2}; \frac{1}{2\gamma_2}\right\} > 0$$

with $\mathbf{M}(\psi) = \begin{pmatrix} M(q) & 0_n \\ 0_n & J \end{pmatrix}$. Therefore $\dot{V}(t) \leq -\gamma^{-1}V(t)$ on $\mathbb{R}_+ \setminus \bigcup_{k \geq 0}[t_0^k, t_f^k]$.

d) There is only one impact during each transition phase since $e = 0$ and with the choice of U_t^B in (20). Therefore $V(t_\infty^k) = V(t_0^{k-}) + \sigma_V(t_0^k) \leq V(\tau_0^k) + \sigma_V(t_0^k)$. We compute now the jump of the Lyapunov function at the impact time t_0^k.

$$\begin{aligned}V(t_0^{k+}) - V(t_0^{k-}) &= \frac{1}{2}\left(s^\top(t_0^{k+})\mathbf{M}(\psi)s(t_0^{k+}) - s^\top(t_0^{k-})\mathbf{M}(\psi)s(t_0^{k-})\right) \\ &\quad + \frac{1}{2}\left(\tilde{\psi}^{\top}(t_0^{k+})\mathcal{K}\tilde{\psi}(t_0^{k+}) - \tilde{\psi}^{\top}(t_0^{k-})\mathcal{K}\tilde{\psi}(t_0^{k-})\right) + \gamma_1\gamma_2\sigma_{\tilde{\psi}^\top\tilde{\psi}}(t_0^k) \end{aligned} \tag{48}$$

Replacing $\tilde{\psi}(t_0^{k+})$ by $\tilde{\psi}(t_0^{k-}) + \sigma_{\tilde{\psi}}(t_0^k)$, the second term of the right hand side of (48) becomes

$$\frac{1}{2}\left(2\tilde{\psi}^{\top}(t_0^{k-})\mathcal{K}\sigma_{\tilde{\psi}}(t_0^k) + \sigma_{\tilde{\psi}}^{\top}(t_0^k)\mathcal{K}\sigma_{\tilde{\psi}}(t_0^k)\right)$$

which is upper bounded by

$$\lambda_{max}(\mathcal{K})(||\tilde{\psi}(t_0^{k-})|| \cdot ||\sigma_{\tilde{\psi}}(t_0^k)|| + \frac{1}{2}||\sigma_{\tilde{\psi}}(t_0^k)||^2)$$

Therefore Lemma 3 and 4 imply that there exists a real positive constant c_1 such that

$$\frac{1}{2}\left(\tilde{\psi}^{\top}(t_0^{k+})\mathcal{K}\tilde{\psi}(t_0^{k+}) - \tilde{\psi}^{\top}(t_0^{k-})\mathcal{K}\tilde{\psi}(t_0^{k-})\right) \leq c_1, \quad \forall k \geq 0 \tag{49}$$

On the other hand

$$s^{\top}(t_0^{k+})\mathbf{M}(\psi)s(t_0^{k+}) - s^{\top}(t_0^{k-})\mathbf{M}(\psi)s(t_0^{k-}) = \sigma_{s_1^{\top}M(q)s_1}(t_0^k) + \sigma_{s_2^{\top}Js_2}(t_0^k)$$

It is easy to see that

$$\sigma_{s_2^{\top}Js_2}(t_0^k) = 2s_2^{\top}(t_0^{k-})J\sigma_{s_2}(t_0^k) + \sigma_{s_2}^{\top}(t_0^k)J\sigma_{s_2}(t_0^k)$$

and using Lemma 3, Lemma 4 and the relation $\sigma_{s_2}(t_0^k) = \sigma_{\dot{\tilde{\theta}}}(t_0^k) + \gamma_2\sigma_{\tilde{\theta}}(t_0^k)$ one deduces that there exist a real positive constant c_2 such that

$$\sigma_{s_2^{\top}Js_2}(t_0^k) \leq c_2, \quad \forall k \geq 0 \tag{50}$$

As proved in [29] there exists a real positive constant c_3 such that

$$\sigma_{s_1^{\top}M(q)s_1}(t_0^k) + \gamma_1\gamma_2\sigma_{\tilde{q}^{\top}\tilde{q}}(t_0^k) \leq c_3, \quad \forall k \geq 0 \tag{51}$$

Finally, Lemma 4 assures the existence of $c_4 \in \mathbb{R}_+$ such that

$$\gamma_1\gamma_2\sigma_{\tilde{\theta}^{\top}\tilde{\theta}}(t_0^k) \leq c_4, \quad \forall k \geq 0 \tag{52}$$

In conclusion, inserting (49), (50), (51) and (52) in (48) one gets

$$V(t_0^{k+}) - V(t_0^{k-}) \leq c_1 + c_2 + c_3 + c_4, \quad \forall k \geq 0 \tag{53}$$

Thus condition **d)** of Proposition 2 is verified for $\rho^* = 1,\ \xi = c_1 + c_2 + c_3 + c_4$ and the closed-loop system (18)-(20) is practically weakly stable with $R = \alpha^{-1}\big(e^{-\gamma(t_f^k - t_\infty^k)}(1 + \xi)\big)$.
Let us consider $\bar{\rho} = \min\{\lambda_{min}(\mathbf{M}(\psi))/2; \gamma_1\gamma_2\}$. Defining $\alpha : \mathbb{R}_+ \mapsto \mathbb{R}_+,\ \alpha(\omega) = \bar{\rho}\omega^2$ we get $\alpha(0) = 0,\ \alpha(||[s(t), \tilde{q}(t)]||) \leq V(t, s, \tilde{q})$ and the proof is finished.

8 Illustrative example

Some numerical results are obtained by simulating the behavior of a planar two-link flexible-joint manipulator in presence of two constraints. As in [29] we impose an admissible domain $\Phi = \{(x, y) \mid y \geq 0,\ 0.7 - x \geq 0\}$. Let us also consider an unconstrained desired trajectory whose orbit is given by the circle $\{(x, y) \mid (x - 0.7)^2 + y^2 = 0.5\}$ that violates both constraints. In other words, the two-link planar manipulator must track a quarter-circle; stabilize on and then follow the line $\Sigma_1 = \{(x, y) \mid y = 0\}$;

stabilize on the intersection of Σ_1 and $\Sigma_2 = \{(x, y) \mid x = 0.7\}$; detach from Σ_1 and follow Σ_2 until the unconstrained circle re-enters Φ and finally take-off from Σ_2 in order to repeat the previous steps. The task representation here is given by (see (4)) $B_{2k} = \emptyset, m_{2k} = 1,\ B_{2k,1} = \{1\}, B_{2k+1} = \{1\},\ m_{2k+1} = 2,\ B_{2k+1,1} = \{1,2\},\ B_{2k+1,2} = \{2\}$.

8.1 Simulation results

Let us say that the quarter-circle is completely tracked in one round. We set the period of each round to 10 seconds and we simulate the dynamics during 6 rounds using the Moreau's time-stepping algorithm of the SICONOS software platform [2]. The numerical values used for the dynamical model are $l_1 = l_2 = 0.5m$, $m_1 = m_2 = 1kg$, $I_1 = I_2 = 0.5kg.m^2$, $J_1 = J_2 = 0.1kg.m^2$ and the impacts are imposed by $\nu = 10$ in (22). The stiffness matrix is defined by $K = diag(2000N/m, 2000N/m)$. We set the controller gains $\gamma_1 = 10$, $\gamma_2 = 1$ and we choose $\nu_1 = 0.1$ (like this we implicitly set τ_0^k see (25)) in order to better point out the deformation of q_d on the transition phases (Figure 2 (left)). In Figure 3 we have shifted backward the desired trajectory on I_2 to highlight that the Lyapunov function at the instant τ_0^k is smaller when k increases.

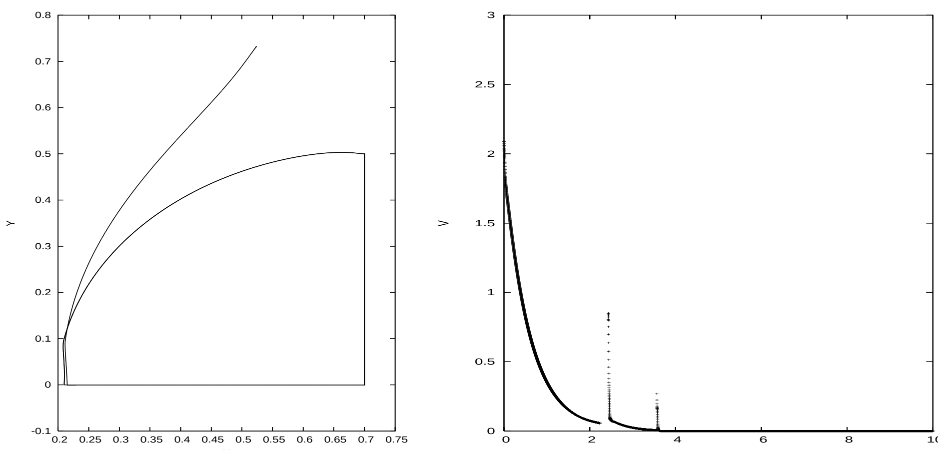

Figure 2: Left:The trajectory of the system during 6 rounds; Right: The variation of the Lyapunov function during the first round.

The behavior of the system during one round is emphasized in Figure 2 (right) and the shape of the control law is depicted in Figure 4.

8.2 The asymptotic dissipation of impacts

In this paragraph we numerically point out that $q_d^*(\cdot)$ converges asymptotically towards a trajectory without impacts. In other words (taking into account (22)), the value of the Lyapunov function at the instant τ_0^k approaches 0 when k tends to infinity. This will obviously lead to lighter impacts when k increases. We also highlight the robustness of the closed-loop system with respect to small perturbations. Precisely, a perturbation will introduce a jump in the variation of the Lyapunov function but the Lyapunov function will continue to decrease outside the impacting transitions, and the

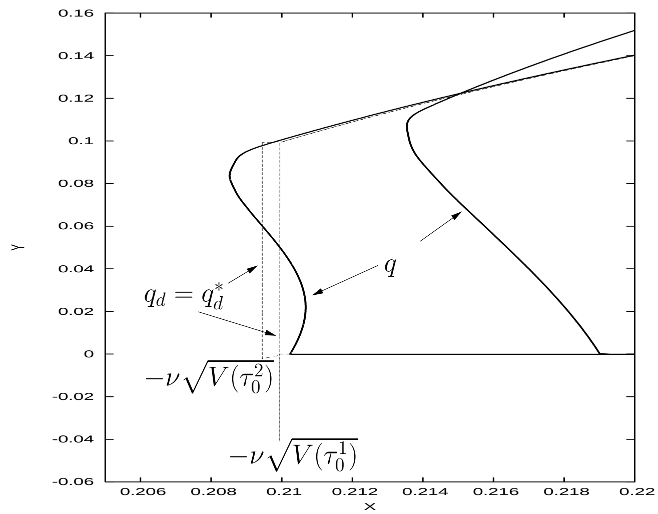

Figure 3: Zoom on the transition phases I_k^1.

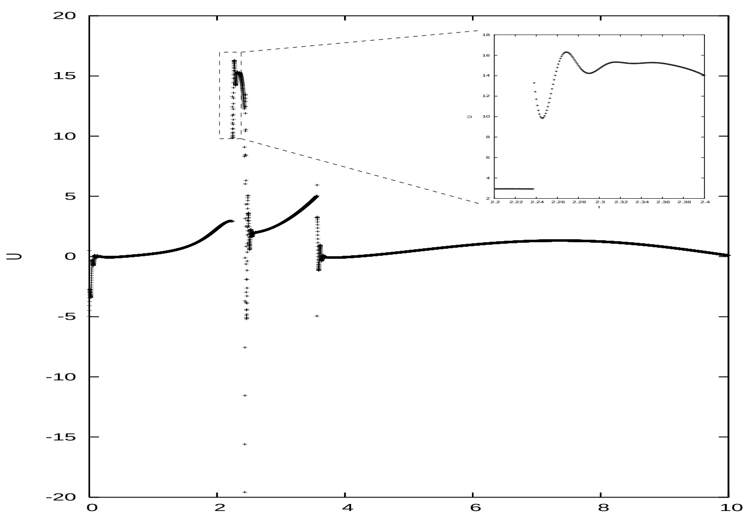

Figure 4: The control law applied to θ_1 during the first round.

tracking process is assured (see Table 1 where some perturbations were introduced in the evolution of the generalized velocities during the free-motion phase Ω_8 of the 5-th round). In Figure 5 the dashed line represents the trajectory of the end-effector after the disturbance has been applied.

Another interesting aspect pointed out in Figure 6 consists of the decrease of the control signal magnitude from one round to the next one. This behavior was expected since the tracking errors become smaller inducing a smaller effort for stabilization.

k	$V(\tau_0^k)$
1	$1.4017 \cdot 10^{-5}$
2	$1.0623 \cdot 10^{-8}$
3	$3.9964 \cdot 10^{-9}$
4	$3.6527 \cdot 10^{-9}$
5	$2.4575 \cdot 10^{-3}$
6	$3.1765 \cdot 10^{-7}$

Table 1: The behavior of $V(\tau_0^k)$ when k increases.

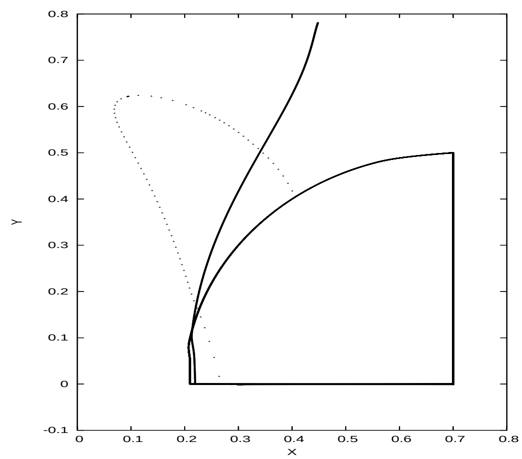

Figure 5: The end-effector evolution with a perturbation introduced during the 5-th round plotted with a dashed line)

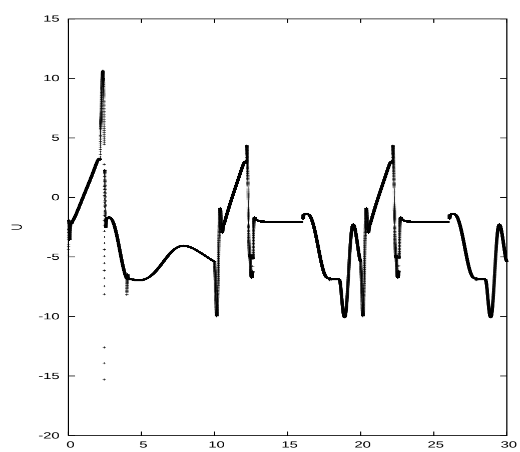

Figure 6: The control signal magnitude decrease from one round to the next one

8.3 The importance of the impacting transition

To better motivate the presence of the impacting transition one considers the admissible domain $\Phi = \{(x, y) \mid y \geq 0\}$ and the unconstrained desired trajectory given by the circle $\{(x, y) \mid (x - 0.4)^2 + y^2 = 0.3\}$ that violates the constraint. We impose a tangential approach of $\partial\Phi$ by setting $\nu = 0$ in (22). As shown in Figure 7 this blocks the tracking process into the transition phase. In fact we can stabilize the system on the constraint (see Figure 8) but the stabilization takes a lot of time and the desired trajectory is not completely tracked. It is noteworthy that the first component of the desired trajectory is frozen until the detection of the first impact.

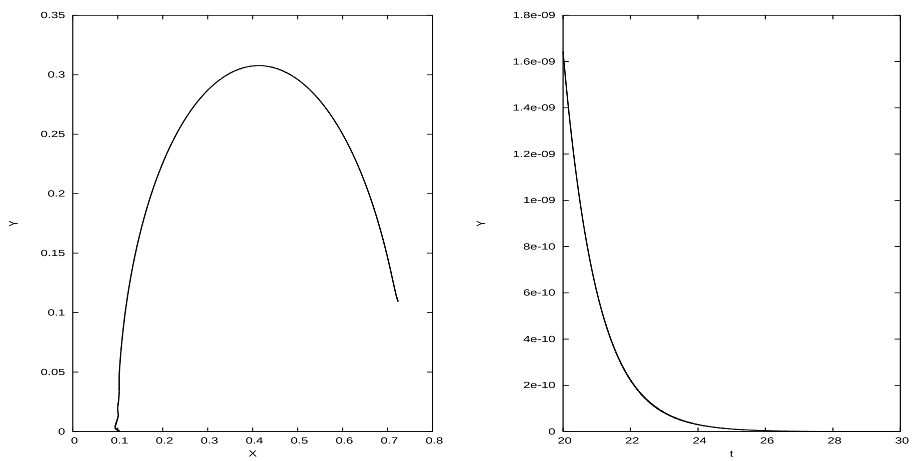

Figure 7: Left: The trajectory of the end-effector when a tangential approach is imposed; Right: Zoom on the variation of the second coordinate of the end-effector in order to prove that the first constraint decreases to the desired value ($y = 0$).

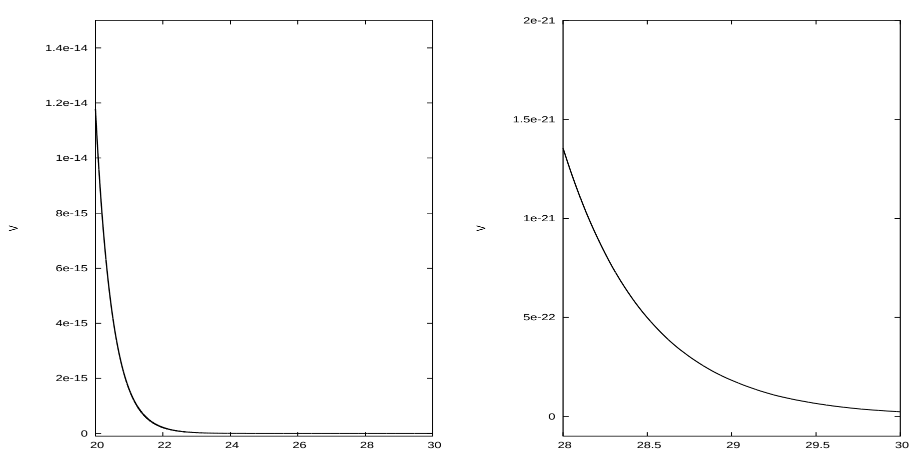

Figure 8: Different zooms show that the Lyapunov function decreases towards 0 when t increases, therefore the system approaches the desired position $(x_d(t), y_d(t)) = (x_d(\tau_0^1), 0)$ but no impact is detected in 30 seconds although the whole trajectory must be tracked in 10 seconds.

8.4 Compensation of flexibilities

As noticed in [11] the control laws designed for rigid systems (the Slotine & Li control and its adaptation for systems with one or multiple constraints [8, 29]) behave well for manipulators with large joint stiffness (see also Figure 9 for the multi-constraint case). It is noteworthy that during the first round the intensity of the impacts is quite big and even small flexibilities degrade the behavior of the system.

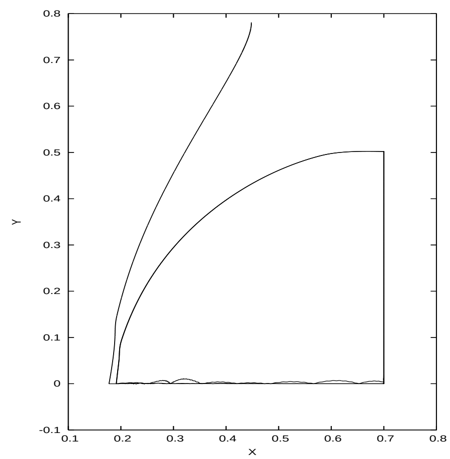

Figure 9: The variation of the end-effector coordinates using the rigid controller when the stiffness matrix is defined by $K = diag(5000N/m, 5000N/m)$.

In order to highlight the importance of flexibilities compensation we keep the numerical values used in the previous Subsection with one exception, the stiffness matrix is defined by $K = diag(200N/m, 200N/m)$. Using the control with no flexibility compensation (named the ”rigid controller”) one obtains a completely deteriorated behavior (see Figure 10). Furthermore, the control signal oscillates very much after the first impact see Figure 11).

On the other hand using the controller designed in this paper the desired trajectory is well tracked (see Figure 12) and the control signal (see Figure 13) is quickly stabilized during the I_k phases.

Numerical simulations show that the Moreau' scheme converges for various values of the stiffness matrix, which proves the reliability of this scheme w.r.t. the stabilization on $\partial\Phi$. Nevertheless, higher flexibilities imply longer stabilization periods and more violent impacts. In order to illustrate the previous affirmation we denote by H the height of the first jump of the second round in the evolution of the Lyapunov function and as noticed before I_3 denotes the first impacting transition of the second round. Recalling that $\lambda[I_3]$ means the Lebesgue measure of the interval I_3, we summarize some simulations data in Table 2.

$K1 = K2$	200	1000	2000
H	0.304	0.058	0.024
$\lambda[I_3]$	$9.2 \cdot 10^{-2}$	$3.9 \cdot 10^{-2}$	$1.9 \cdot 10^{-2}$

Table 2: Higher flexibilities imply longer stabilization periods and more violent impacts.

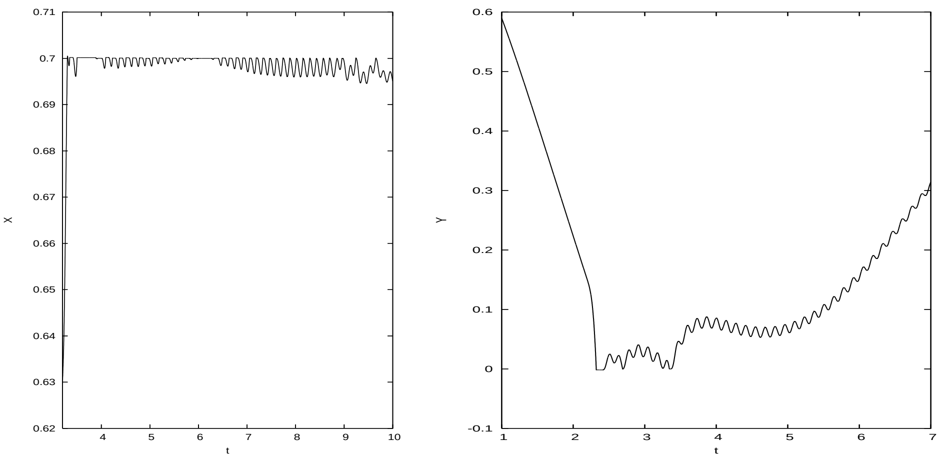

Figure 10: The variation of the end-effector coordinates using the rigid controller ($K = diag(200N/m, 200N/m)$).

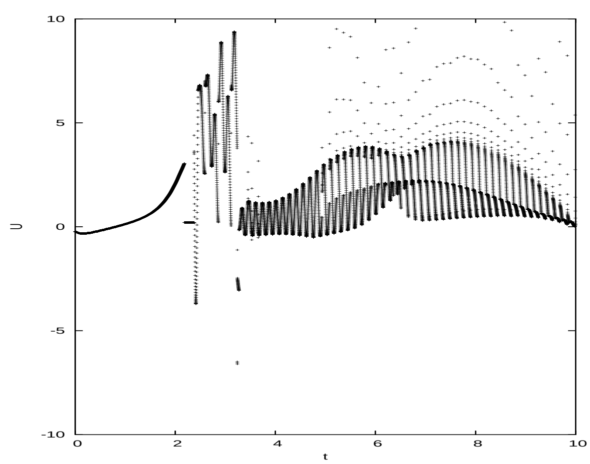

Figure 11: The rigid control applied to θ_1 during the first round ($K = diag(200N/m, 200N/m)$).

8.5 Numerical results for the restitution coefficient within $(0, 1)$

The simulations presented in the sequel encourage us to go further and expect that the control law designed in this paper can be used not only for the plastic impacts case but also when $e \in (0, 1)$. In order to have the possibility to compare the results we use the numerical values introduced at the beginning of this Section.

Since the impacting transition for $e \in (0, 1)$ does not reduce to one instant, we plot in Figure 14 the variation of y and y_d^* in order to better illustrate the definition (22). It is worth to recall here that

$$y_d(t) = y_d^*(t), \quad \forall t \in \mathbb{R}_+ \setminus \{t \in \mathbb{R}_+ \mid y_d^*(t) = -\nu V(\tau_0^k)\}$$
$$y_d(t) = 0, \quad \forall t \in \{t \in \mathbb{R}_+ \mid y_d^*(t) = -\nu V(\tau_0^k)\}$$

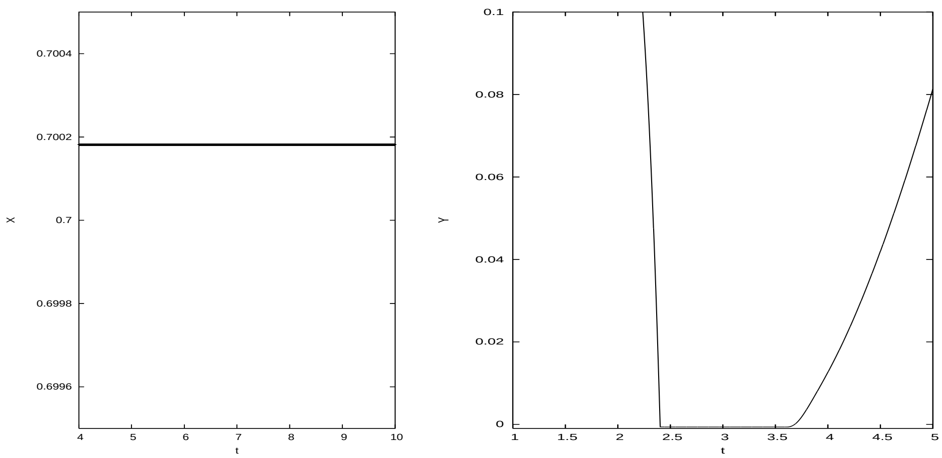

Figure 12: The variation of the end-effector coordinates using the control (19) (20) ($K = diag(200N/m, 200N/m)$).

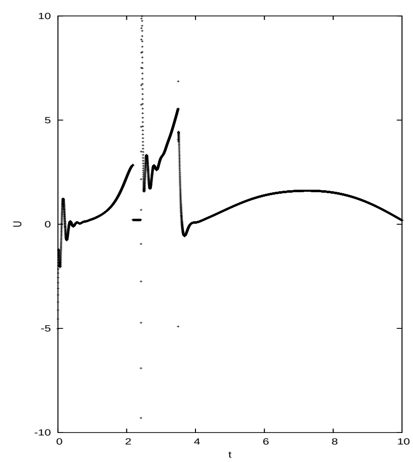

Figure 13: The control law (19) (20) applied to θ_1 during the first round ($K = diag(200N/m, 200N/m)$).

We also note that the evolution of q_d^* may be used (as in Figure 3) to point out the evolution of $V(\tau_0^k)$ when k increases.

As we can see in Figure 15 even for $e = 0.9$ the behavior of the systems does not deteriorate very much and the desired trajectory is well tracked especially starting with the second round.

Since the restitution coefficient was set to a high value ($e = 0.9$) and the tracking error during the first round is quite big, the behavior of the system during the first transition phase is degraded. Some practical application could demand a more accurate tracking and an end-effector trajectory as in Figure 15 may not be acceptable. In order to improve the accuracy of tracking we have two possibilities. The first one consists of increasing the period of each round, which implies a longer first free-motion phase and consequently a smaller tracking error at the instant τ_0^k (see (22)). Numerical simulation

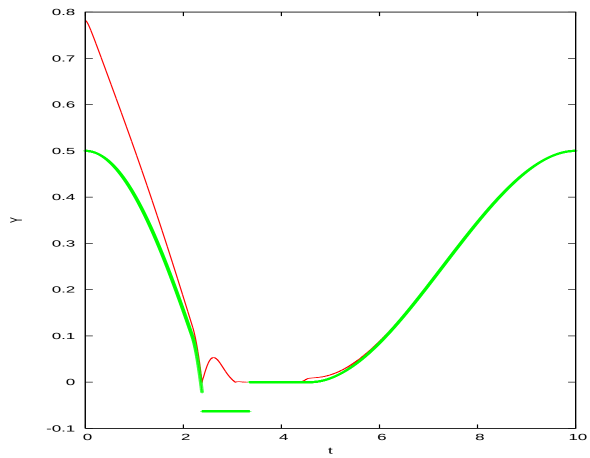

Figure 14: The evolution of y (red) and y_d^* (green) during the first round.

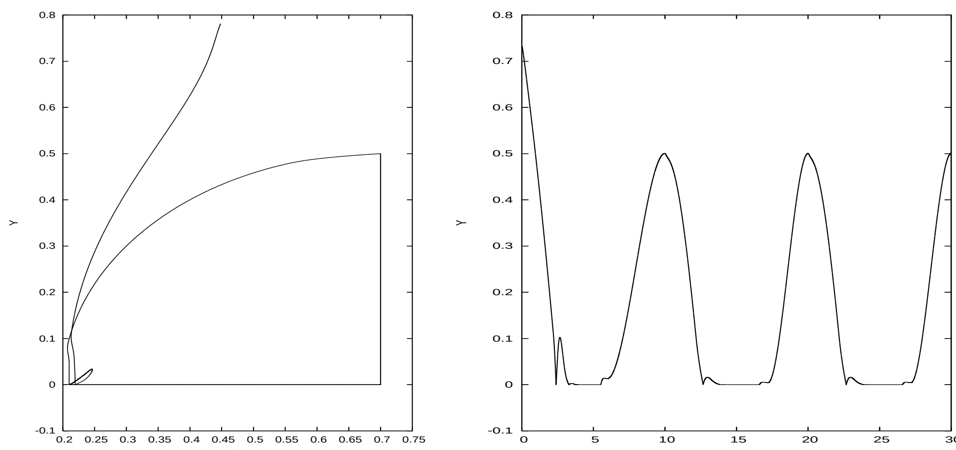

Figure 15: Left: The trajectory of the end-effector when the restitution coefficient is set to $e = 0.9$; Right: The variation of y when the restitution coefficient is set to $e = 0.9$.

shows that for a period of 20 seconds per round, the system's trajectory and the control signal are seriously improved (see Figure 16).

The second way to improve the accuracy of the tracking consists of adjusting better the controller gain. As shown in Figure 17 a larger value of γ_2 (which corresponds to a larger value of the spring stiffness entering the control, see [11, 29] for more details) improves the system's trajectory.

It is noteworthy that a larger value of γ_2 implies an increase of the control signal magnitude (see Figure 18), which may not be acceptable in practice due to saturation.

In the sequel one denotes by N_i^1 and N_i^2 the number of impacts captured using a time-step $h = 10^{-3}$ during the transition phases I_1 and I_2 respectively. Let us also denote by H the height of the first jump in the evolution of the system's trajectory. Then, as expected, N_i^1, N_i^2 and H increase when the restitution coefficient increases from 0 to 1(see Table 3 for numerical values).

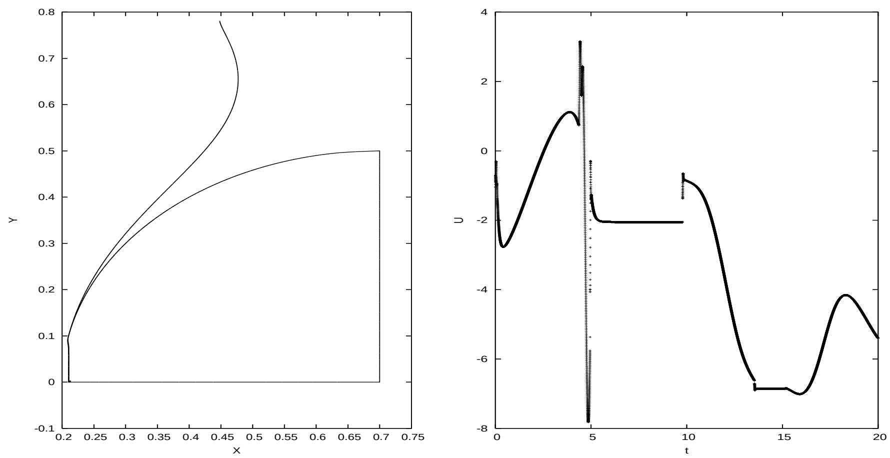

Figure 16: Left: The trajectory of the end-effector when the restitution coefficient is set to $e = 0.9$ and the duration of each round is 20 seconds; Right: The control law applied to θ_1 during the first round when the restitution coefficient is set to $e = 0.9$ and the duration of each round is 20 seconds.

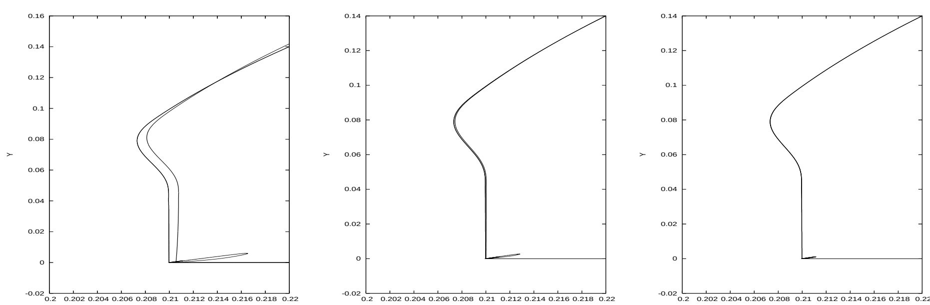

Figure 17: Zoom on transition phases I_k^1 when $\gamma_2 = 2$, $\gamma_2 = 3$ and $\gamma_2 = 4$, respectively.

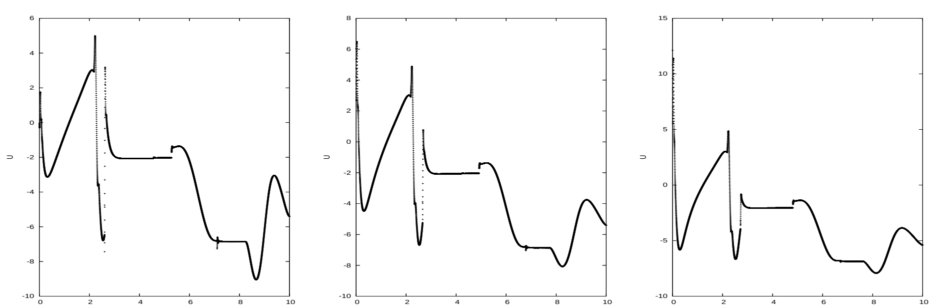

Figure 18: The control signal applied to θ_1 during the first round when $\gamma_2 = 2$, $\gamma_2 = 3$ and $\gamma_2 = 4$, respectively.

In [29] we have proved that the Lyapunov function associated to the rigid-joint system may have a positive first jump for each transition phase, but all the other jumps are negative. As can be seen in Figure 19 (right) for the flexible-joint system one has

e	0.5	0.7	0.9
N_i^1	9	15	35
N_1^2	7	11	30
H	0.044	0.072	0.104

Table 3: The behavior of N_i^1, N_i^2 and H with respect to the restitution coefficient e.

multiple positive jumps in the evolution of the Lyapunov function. Nevertheless the simulations reveal an almost decreasing Lyapunov function characterizing a weakly stable system (see Figure 19 (left)).

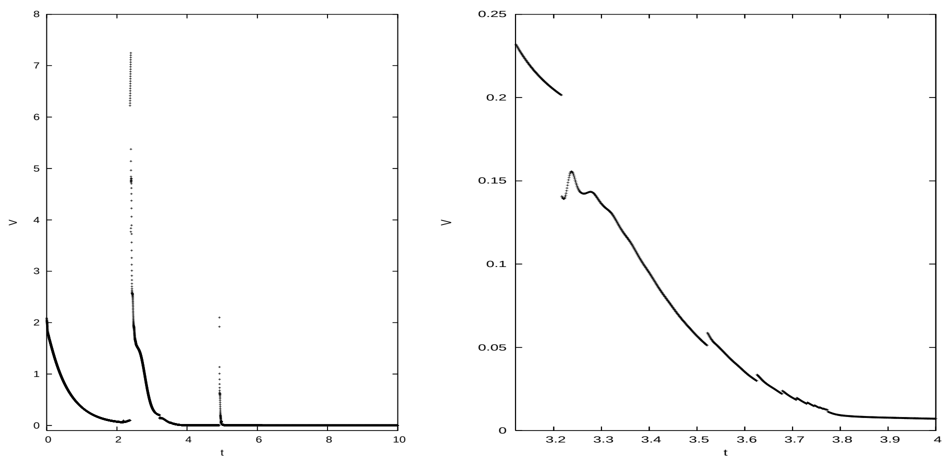

Figure 19: Left: The variation of the Lyapunov function during one round ($e = 0.7$); Right: Zoom on the first transition phase

9 Conclusions

In this paper we have proposed a solution for the trajectory tracking control of complementarity nonsmooth Lagrangian systems with flexible joints. All the ingredients entering the dynamics (desired trajectories, desired contact forces, exogenous instants playing a role in the definition of the control law) are explicitly defined. It is noteworthy that the flexible-joint case is more difficult than the rigid-joint case since the backstepping procedure involves some exogenous trajectories that are defined as nonlinear functions of states and other exogenous signals. Therefore, the ”passivity-based” Lyapunov function has jumps that are more difficult to characterize. Numerical simulations, done with the SICONOS software platform, illustrate on one hand the necessity and the robustness of the control scheme proposed in the paper, and on the other hand they encourage us to attempt the extension of the study to the case where the restitution coefficient belongs to $[0, 1)$.

References

[1] Acary, V. and Brogliato, B.: *Numerical Methods for Nonsmooth Dynamical Systems*, Lecture Notes in Applied and Computational Mechanics, vol **35**, Springer-Verlag, Berlin Heidelberg, (2008).

[2] Acary, V. and Pérignon, F.: *An introduction to* SICONOS, INRIA Technical report RT 340, (2007) SICONOS open-source software available at: http://siconos.gforge.inria.fr/.

[3] Albu-Schaffer, A., Ott, C.; Hirzinger, G: *A passivity based Cartesian impedance controller for flexible joint robots - part II: full state feedback, impedance design and experiments*, Proceedings ICRA '04, IEEE International Conference on Robotics and Automation, vol.3, pp.2666 - 2672, April 26-May 1, (2004).

[4] Ballard, P.: *The dynamics of discrete mechanical systems with perfect unilateral constraints*, Arch. Rational Mech. Anal. **154**, 199-274, (2000).

[5] Ballard, P.: *Formulation and well-posedness of the dynamics of rigid body systems with perfect unilateral constraints*, Phil. Trans. R. Soc. Lond. **A359**, 2327-2346, (2001).

[6] Bentsman, J. and Miller, B.: *Generalized solutions in systems with active unilateral constraints*, Nonlinear Anal., Hybrid Syst. 1, No. 4, 510-526 (2007).

[7] Bentsman, J. and Miller, B.: *Dynamical systems with active singularities of elastic type: A modeling and controller synthesis framework*, IEEE Transactions on Automatic Control, vol.52, no 1, pp.39-55, January (2007).

[8] Bourgeot, J.-M. and Brogliato, B.:*Tracking control of complementarity lagrangian systems*, International Journal of Bifurcation and Chaos, **15**(6), 1839-1866, (2005).

[9] Brogliato, B.: *Absolute stability and the Lagrange-Dirichlet theorem with monotone multivalued mappings*, Systems and Control Letters, vol.51, 343-353, 2004.

[10] Brogliato, B.: *Nonsmooth Mechanics*, Springer CCES, London, (1999), 2nd Ed.

[11] Brogliato, B., Lozano, R., Maschke, B. and Egeland, O.: *Dissipative Systems Analysis and Control. Theory and Applications*, Springer CCES, London, (2007), 2nd Ed.

[12] Brogliato, B., Niculescu, S.-I., Orhant, P.: *On the control of finite-dimensional mechanical systems with unilateral constraints*, IEEE Trans. Autom. Contr. **42**(2), 200-215, (1997).

[13] Brogliato, B., Ortega, R., Lozano, R.: *Global tracking controllers for flexible-joint manipulators: a comparative study*, Automatica, **31**(7), 941-956, (1995).

[14] Casagrande, D., Astolfi, A., Parisini, T.: *Golbal asymptotic stabilization of the attitude and the angular rates of an underactuated non-symmetric rigid body*, Automatica, vol.44, no 7, pp.1781-1789 (2008).

[15] Dzonou, R. and Monteiro Marques, M.D.P.:*A sweeping process approach to inelastic contact problems with general inertia operators*, European Journal of Mechanics - A/Solids, **26**(3), 474-490, (2007).

[16] Facchinei, F. and Pang, J.S.: *Finite-dimensional Variational Inequalities and Complementarity Problems*, Springer Series in Operations Research, New-York, (2003).

[17] Galeani, S., Menini, L., Potini, A. and Tornambè, A.: *Trajectory tracking for a particle in elliptical billiards*, International Journal of Control, vol. **81**(2), 189-213, (2008).

[18] Glocker, C.: *Set Valued Force Laws: Dynamics of Non-Smooth Systems* Lecture Notes in Applied Mechanics, Vol.1, Springer, (2001).

[19] Lee, E. and Park, J. and Loparo, K.A. and Schrader, C.B. and Chang, P.H.: *Bang-bang impact control using hybrid impedance/time-delay control*, IEEE/AMSE Transactions on Mechatronics, vol.**8**, No.2, 272-277, (2003).

[20] Leine, R.I. and van de Wouw, N.: *Stability properties of equilibrium sets of non-linear mechanical systems with dry friction and impact*, Nonlinear Dynamics, Vol **51**(4), 551-583, (2008).

[21] Leine, R.I. and van de Wouw, N.: *Uniform convergence of monotone measure differential inclusions: with application to the control of mechanical systems with unilateral constraints*, Int. Journal of Bifurcation and Chaos, vol.18, no 5, pp.1435-1457, (2008).

[22] Leine, R.I. and van de Wouw, N.: *Stability and Convergence of Mechanical Systems with Unilateral Constraints*, Lecture Notes in Applied and Computational Mechanics, vol.36, Springer Verlag Berlin Heidelberg, (2008).

[23] Mabrouk, M.: *A unified variational model for the dynamics of perfect unilateral constraints*, European Journal of Mechanics A/ Solids, **17**(5), 819-842, (1998).

[24] McClamroch, N. and Wang, D.: *Feedback stabilization and tracking of constrained robots*, IEEE Trans. Autom. Contr. **33**, 419-426, (1988).

[25] Menini, L. and Tornambè, A.: *Asymptotic tracking of periodic trajectories for a simple mechanical system subject to nonsmooth impacts*, IEEE Trans. Autom. Contr. **46**, 1122-1126, (2001).

[26] Menini, L. and Tornambè, A: *Exponential and BIBS stabilisation of one degree of freedom mechanical system subject to single non-smooth impacts*, IEE Proc.- Control Theory Appl. Vol.**148**, No. 2, 147-155, (2001).

[27] Menini, L. and Tornambè, A: *Dynamic position feedback stabilisation of multidegrees-of-freedom linear mechanical system subject to nonsmooth impacts*, IEE Proc.- Control Theory Appl. Vol.**148**, No. 6, 488-496, (2001).

[28] Miller, B. and Bentsman, J.: *Optimal control problems in hybrid systems with active singularities*, Nonlinear Anal., Theory Methods Appl. 65, No. 5 (A), 999-1017 (2006).

[29] Morărescu, I.-C. and Brogliato, B: *Passivity-based tracking control of multiconstraint complementarity Lagrangian systems*, IEEE Conference on Decision and Control, Cancun, Mexico, December 9-11 (2008). See also http://hal.inria.fr/docs/00/27/62/64/PDF/RR-6483.pdf

[30] Moreau, J. J: *Unilateral contact and dry friction in finite freedom dynamics*, Nonsmooth Mechanics and Applications, CISM Courses and Lectures, Vol. **302** (Springer-Verlag), (1988).

[31] Pagilla, P.R.: *Control of contact problem in constrained Euler-Lagrange cystems*, IEEE Transactions on Automatic Control, vol.**46**, No. 10, 1595-1599, (2001).

[32] Pagilla, P.R. and Yu, B. *An experimental study of planar impact of a robot manipulator*, IEEE/ASME Transactions on Mechatronics, vol.**9**, No. 1, 123-128, (2004).

[33] Sekhavat, P. and Sepehri, N. and Wu, Q.: *Impact stabilizing controller for hydraulic actuators with friction: Theory and experiments*, Control Engineering Practice, vol.**14**, 1423-1433, (2006).

[34] Tornambé, A.: *Modeling and control of impact in mechanical systems: Theory and experimental results*, IEEE Transactions on Automatic Control, vol.**44**, No. 2, 294-309, (1999).

[35] van Vliet, J. and Sharf, I. and Ma, O.: *Experimental validation of contact dynamics simulation of constrained robotic tasks*, International Journal of Robotics Research, vol.**19**, No.12, 1203-1217, (2000).

[36] Volpe, R. and and Khosla, P.: *A theoretical and experimental investigation of impact control for manipulators*, International Journal of Robotics Research, vol.**12**, No.4, 351–365, (1993).

[37] S. Wolf, G. Hirzinger: *A new variable stiffness design: matching requirements of the next robot generation*, Proceedings of the IEEE Int. Conf. on Robotics and Automation, Pasadena, CA, USA, May 19-23, pp.1741-1746, (2008).

[38] Xu, W.L.and Han, J.D. and Tso, S.K.: *Experimental study of contact transition control incorporating joint acceleration feedback*, IEEE/ASME Transactions on Mechatronics, vol.**5**, No.3, 292-301, (2000).

[39] Yu, B. and Pagilla, P.R.: *Design and implementation of a robust switching control scheme for a class of constrained robot tasks*, International Journal of Systems Science, vol.**37**, No. 5, 303-321, (2006).

Centre de recherche INRIA Grenoble – Rhône-Alpes
655, avenue de l'Europe - 38334 Montbonnot Saint-Ismier (France)

Centre de recherche INRIA Bordeaux – Sud Ouest : Domaine Universitaire - 351, cours de la Libération - 33405 Talence Cedex
Centre de recherche INRIA Lille – Nord Europe : Parc Scientifique de la Haute Borne - 40, avenue Halley - 59650 Villeneuve d'Ascq
Centre de recherche INRIA Nancy – Grand Est : LORIA, Technopôle de Nancy-Brabois - Campus scientifique
615, rue du Jardin Botanique - BP 101 - 54602 Villers-lès-Nancy Cedex
Centre de recherche INRIA Paris – Rocquencourt : Domaine de Voluceau - Rocquencourt - BP 105 - 78153 Le Chesnay Cedex
Centre de recherche INRIA Rennes – Bretagne Atlantique : IRISA, Campus universitaire de Beaulieu - 35042 Rennes Cedex
Centre de recherche INRIA Saclay – Île-de-France : Parc Orsay Université - ZAC des Vignes : 4, rue Jacques Monod - 91893 Orsay Cedex
Centre de recherche INRIA Sophia Antipolis – Méditerranée : 2004, route des Lucioles - BP 93 - 06902 Sophia Antipolis Cedex

Éditeur
INRIA - Domaine de Voluceau - Rocquencourt, BP 105 - 78153 Le Chesnay Cedex (France)
http://www.inria.fr
ISSN 0249-6399